Soil–climate interactions drive above-ground biomass in the Caatinga, the largest Neotropical seasonally dry tropical forest

Alexandre T. Brunello[1,36*], Domingos Cardoso[2,3], Peter W. Moonlight[4,5], Ítalo A. C. Coutinho[6], John Cunha[7], Mário M. do Espírito Santo[8], Magna S. B. de Moura[9,10], Luciano P. de Queiroz[11], Rubens M. dos Santos[12], Tiina Särkinen[4], Raquel C. Miatto[1], Tony C. de S. Oliveira[34,35], Cidney Bezerra[13], Marcelo Mizushima[11], Ana Carla M. M. Aquino[14], Moabe F. Fernandes[15], Desirée M. Ramos[16], Valdemir F. da Silva[17], Priscyla M. S. Rodrigues[18], Jhonathan de O. Silva[18], Alberto J. F.Castro[19], Rômulo Menezes[20], Francisca S. Araújo[21], Patrícia Morellato[16], Laura Borma[22], Emerson R. Almeida[23], Rodolfo L. B. Nóbrega[24,25], Rodolfo M. S. Souza[26], Maria J. N. Rodal[17], Vinícius A. Maia[33], Anne Verhoef[27], Elmar Veenendaal[28], R. Toby Pennington[4,29], Oliver L. Phillips[30], Carlos A. N. Quesada[31], Jon Lloyd[32], Tomas F. Domingues[1*]

[1]Universidade de São Paulo (USP), Faculdade de Filosofia, Ciências e Letras de Ribeirão Preto (FFCLRP), Departamento de Biologia, Av. dos Bandeirantes, 3900, Monte Alegre, Ribeirão Preto, SP, Brazil

[2]Instituto de Pesquisas Jardim Botânico do Rio de Janeiro, Rua Pacheco Leão, 915, Rio de Janeiro, RJ, Brazil

[3]Instituto de Biologia, Universidade Federal da Bahia, Rua Barão de Jeremoabo, s.n., Ondina, Salvador, BA, Brazil

[4]Royal Botanic Garden Edinburgh, 20a Inverleith Row, Edinburgh EH3 5LR, UK

[5]Botany, School of Natural Sciences, Trinity College Dublin, Dublin 2, Ireland

[6]Universidade Federal do Ceará, Centro de Ciências, PPGS−Programa de Pós-graduação em Sistemática, Uso e Conservação da Biodiversidade, Av. da Universidade, 2853, Benfica, Fortaleza, CE, Brazil

[7]Centro de Tecnologia e Recursos Naturais (CTRN), Universidade Federal de Campina Grande, Av. Aprígio Veloso, 882, Bodocongó, Campina Grande, PB, Brazil

[8]Departamento de Biologia Geral/CCBS, Universidade Estadual de Montes Claros, Av. Rui Braga, s/n, Vila Mauricéia, Montes Claros, MG, Brazil

[9]Empresa Brasileira de Pesquisa Agropecuária, Embrapa Semiárido, BR 428, Km 152, Zona Rural, Petrolina, PE, Brazil

[10]Empresa Brasileira de Pesquisa Agropecuária, Embrapa Agroindústria Tropical, Rua Dra. Sara Mesquita, 2270, Pici, Fortaleza, CE, Brazil

[11]Departamento de Ciências Biológicas, Universidade Estadual de Feira de Santana, Av. Transnordestina, s/n, Novo Horizonte, Feira de Santana, BA, Brazil

[12]Laboratório de Fitogeografia e Ecologia Evolutiva, Universidade Federal de Lavras, Campus Universitário, Lavras, MG, Brazil

[13]Unidade Acadêmica de Garanhuns, Universidade Federal Rural de Pernambuco, Av. Bom Pastor, s/n, Boa Vista, Garanhuns, PE, Brazil

[14]Laboratório de Ecologia, Manejo e Conservação de Fauna, Departamento de Ciências Florestais, ESALQ/USP, Av. Pádua Dias, 11, Agronomia, Piracicaba, SP, Brazil

[15]Royal Botanic Gardens, Kew, Richmond, TW9 3AE, UK

[16]São Paulo State University (UNESP), Center for Research on Biodiversity Dynamics and Climate Change, Phenology Lab and Department of Biodiversity, Institute of Bioscience, Av. 24-A, 1515, Bela Vista, Rio Claro, SP, Brazil

[17]Departamento de Fitotecnia e Ciências Ambientais, Universidade Federal da Paraíba (UFPB), Areia, PB, Brazil

[18]Colegiado de Ecologia, Campus Senhor Do Bonfim-BA, Universidade Federal Do Vale Do São Francisco (UNIVASF), Rua Tomaz Guimarães, s/n, Santos Dumont, Senhor do Bonfim, BA, Brazil

[19]Universidade Federal do Piauí, Programa de Biodiversidade do Trópico Ecotonal do Nordeste (BIOTEN), Departamento de Biologia, Centro de Ciências da Natureza, Campus da Ininga, Av. Universitária, s/n, Ininga, Teresina, PI, Brazil

[20]Department of Nuclear Energy, Federal University of Pernambuco, Av. Prof. Luís Freire, 1000, Recife, PE, Brazil

[21]Department of Biology, Building 906, Federal University of Ceará, Av. Humberto Monte, s/n, Pici, Fortaleza, CE, Brazil

[22]Divisão de Impacto, Adaptação e Vulnerabilidade - DIIAV/INPE, Av. dos Astronautas, 1758, Jardim da Granja, São José dos Campos, SP, Brazil

[23]Instituto de Geografia, Geociências e Saúde Coletiva (IGESC), LMG 746, Km1, Monte Carmelo, MG, Brazil, LMG

[24]University of Bristol, School of Geographical Sciences, Bristol, UK

[25]University of Bristol, Cabot Institute for the Environment, University Road, Bristol BS8 1SS, UK

[26]Environmental Modeling, Texas A&M Transportation Institute, 1111 RELLIS Parkway, Bryan, TX, USA

[27]Department of Geography and Environmental Science, The University of Reading, Whiteknights, PO Box 217, Reading RG6 6AH, UK

[28]Plant Ecology and Nature Conservation, Wageningen University and Research, Droevendaalsesteeg 3a, Wageningen, The Netherlands

[29]Geography, University of Exeter, Laver Building, North Park Road, Exeter EX4 4QE, UK

[30]University of Leeds, School of Geography, Woodhouse Lane, Leeds LS2 9JT, U.K

[31]Instituto Nacional de Pesquisas da Amazônia (INPA), Avenida André Araújo, 2936 - Petrópolis, Manaus, AM, Brazil

[32]School of Biological Sciences, The University of Western Australia, 35 Stirling Highway, Crawley, Perth, WA, Australia

[33]Departamento de Ciências Florestais, Universidade Federal de Lavras, Campus Universitário, P.O. Box 3037, Lavras, MG, Brazil

[34]Institute of Bio- and Geosciences, IBG-2: Plant Sciences, Forschungszentrum Jülich GmbH, 52428 Jülich, Germany

[35]Faculty of Communication and Environment, Rhine-Waal University of Applied Sciences, 47475 Kamp-Lintfort, Germany

[36]Laboratory of Isotope Ecology, Center for Nuclear Energy in Agriculture (CENA), University of São Paulo, Piracicaba, SP, Brazil

Corresponding authors: A. T. Brunello (brunelloflorestal@gmail.com) and T. F. Domingues (tomas@ffclrp.br)

Abstract

Background and Aims: Soil properties are key drivers of vegetation structure, yet their influence on above-ground woody biomass (AGB_W) in seasonally dry tropical forests (SDTFs) remains underexplored, particularly at larger scales. This gap is evident in the Caatinga, Latin America's largest SDTF, known for its biodiversity and carbon storage potential. We investigated relationships among soil, climate, and vegetation properties to understand accumulation patterns of AGB_W in SDTFs.

Methods: We used standardised soil and vegetation data from 29 research plots spanning diverse geological and floristic conditions. Linear mixed models and multi-model inference were applied to analyse relationships between AGB_W and environmental variables, including soil texture, fertility, plant-available soil water, mean annual precipitation (MAP), temperature, and climatic water deficit (CWD). Structural equation modelling (SEM) was utilised to assess how environmental variables influenced community-weighted maximum stem diameter, wood density, functional richness, and their combined effects on AGB_W.

Results: AGB_W was influenced by MAP, soil fertility, maximum plant-available soil water, and CWD. SEM indicated that soil nutrient availability shaped community functional traits, reflecting trade-offs between growth and water-use strategies. In turn, species' maximum stem diameter and, to a lesser extent, functional richness positively influenced AGB_W, underscoring the role of soil-mediated functional traits in determining biomass.

Conclusion: AGB_W in the Caatinga is shaped by soil, climate, and their interactions, with soil properties exerting strong effects on community functional diversity. Our findings highlight patterns of functional trait variability and biomass storage, offering insights for biodiversity conservation and carbon sequestration in SDTFs under global environmental change.

Keywords: Brazilian semi-arid, carbon stocks, drylands, functional traits, global change, dryland soils

Introduction

Above-ground woody biomass (AGB_W) is a key component of the carbon cycle in forest systems, as it integrates productivity, recruitment, and mortality dynamics (Lloyd et al. 2009). Although seasonally dry tropical forests (SDTFs) typically have lower AGB_W stocks than their wetter counterparts, they are important carbon reservoirs due to their widespread distribution in the tropics (Glenday 2008; Roa-Fuentes et al. 2012; Corona-Núñez et al. 2018). While this work focuses on AGB_W, which typically accounts for approximately 60–70% of the total biomass per unit area in SDFTs, the remaining portion is represented by below-ground biomass (BGB) (Murphy and Lugo 1986; Menezes et al. 2021), underscoring the importance of both pools for carbon storage in these ecosystems. Once estimated to comprise 42% of all subtropical and tropical forests (Murphy and Lugo 1986), SDTFs are now experiencing significant declines, with an 11.4% global loss in cover from 2001 to 2020 (Ocón et al. 2021). These ecosystems have been recognised as highly diverse yet threatened (Miles et al. 2006; DRYFLOR 2016). The Caatinga region in Brazil, which hosts the largest continuous expanse of SDTF in Latin America, harbours substantial biodiversity (Queiroz et al. 2017; Fernandes et al. 2020; Londe et al. 2023) and has significant carbon storage potential (Castanho et al. 2020), highlighting its ecological importance. However, like other neotropical SDTFs, the Caatinga is under threat from various pressures and lacks conservation efforts (Oliveira et al. 2012; DRYFLOR 2016). The Caatinga SDTFs have long faced anthropogenic pressures, including firewood and charcoal extraction, cattle raising and overgrazing, and slash-and-burn agriculture (Andrade 1977; Araujo et al. 2023). These activities have pushed many previously forested areas towards ecological thresholds, with only 11% of the original forest coverage remaining, while some areas are desertified or at risk of desertification (Araujo et al. 2023). Despite the overwhelming influence of human activities on AGB_W distribution in the region, it remains crucial to investigate how environmental factors shape

AGB_W in structurally mature stands, as these can offer insights into potential AGB_W accumulation under semi-natural conditions.

Despite the likely influence of both climate and soils on AGB_W, research has primarily focused on climatic factors, with soil properties often underrepresented. Among climatic variables, mean annual precipitation is widely recognised as a primary driver of AGB_W, and many studies have associated biomass accumulation with rainfall gradients (e.g., Brown and Lugo 1982; Becknell et al. 2012; Castanho et al. 2020). However, plant water availability is also influenced by evapotranspiration, precipitation seasonality, and soil properties. While the positive correlation between mean annual precipitation and AGB_W is well-reported, few studies have taken soil attributes, such as soil texture, clay mineralogy, and nutrient levels, into account, mainly due to incompatible sampling and analysis protocols or simply due to the absence of soil data (Becknell et al. 2012; Santos et al. 2023). This gap in knowledge limits our understanding of how environmental drivers interact to shape AGB_W in SDTFs, particularly in the spatially complex Caatinga region.

In this region, distinct geological substrates have given rise to a variety of Reference Soil Groups (RSGs, the highest categorical level in the WRB–FAO soil classification), ranging from nutrient-rich shallow soils overlying carbonate rocks to fertile, fine-textured shallow soils over crystalline basements, to less fertile, deeper soils developed from sedimentary deposits (Sampaio 1995; Oliveira 2011). Earlier studies have highlighted the significant role of soil properties in shaping vegetation structure and floristic composition in Brazilian dry forests (e.g., Ratter et al. 1973; 1978; Furley and Ratter 1988). In the Caatinga, soil properties have been linked to local variations in structural and floristic diversity (e.g., Souza et al. 2019; Maia et al. 2020). At the regional scale, the combination of soil properties and climate attributes has been shown to more effectively predict differences in vegetation physiognomies than either soil or climate separately (Oliveira et al. 2019).

The relationship between vegetation and environmental conditions can also be explored through the lens of functional attributes, and associated community functional properties, such as community-weighted mean maximum stem diameter (CWM_{DMAX}), wood density (CWM_{WD}), and their derived functional richness (F_{RIC}), i.e., the range and diversity of single or combined traits within each community. These traits have been shown to influence stand-level biomass and productivity in dry ecosystems (Prado-Junior et al. 2016). In their

study, Prado-Junior et al. (2016) tested contrasting ecological hypotheses to explain biomass accumulation patterns in SDTFs, including the 'biomass ratio hypothesis' (Grime 1998), which suggests that the dominant traits in a community exert the greatest influence on stand-level ecosystem properties; the 'niche complementarity hypothesis' (Tilman et al., 1999), which proposes that species can coexist by using resources differently, thereby reducing competition; and the 'soil fertility hypothesis' (Pastor et al. 1984), comprehensively tested in this study.

Here, we use a *Space-for-Time* approach (Pickett, 1989), which involves examining spatial variation across environmental gradients as a proxy for temporal ecological changes. This approach is particularly useful in the Caatinga, where long-term monitoring studies are limited, but pronounced environmental heterogeneity may reflect ecosystem development over time or responses to long-term drivers. By comparing plots distributed across climatic and edaphic gradients, we aim to infer how these factors shape current patterns of biomass accumulation and functional diversity.

Specifically, we address the following research questions: (1) How do soil, climate, and their potential interactions modulate patterns of biomass accumulation in the Caatinga region? (2) How does soil influence stand-level functional properties, such as wood density, maximum stem diameter, and the associated functional richness? (3) How do these functional properties affect stand-level above-ground woody biomass? By integrating standardised soil and vegetation data from 29 research plots across the Brazilian Caatinga, this study seeks to deepen our understanding of the environmental and functional drivers of biomass in SDTFs, offering valuable insights for the conservation and management of these ecosystems in the context of global change.

Material and Methods

Study sites

Data used in this study were compiled from 29 study plots established by the *Nordeste Project* (see Acknowledgements and Funding for further details). These plots are distributed across the Brazilian Caatinga region (Table 1, Fig. 1), encompassing seven reference soil groups (RSGs), three geological substrate types, and distinct mineral assemblages. These mineral assemblages are represented by high-activity clay soils (HAC), low-activity clay soils (LAC), and highly sandy soils (Arenic), as described below. The sampled soils vary from

shallow, slightly weathered soils mostly developed from crystalline rocks (S_{CRY}) to much deeper, highly weathered soils overlying sedimentary substrates (S_{SED}), including two study plots located in the Quaternary dunes of the middle *São Francisco River*. Additionally, the sampling included three vegetation stands on soils derived from carbonate rocks (S_{CAR}), characterised by distinctive properties such as elevated calcium (Ca) and phosphorus (P) levels, and neutral to basic soil pH. Examples of sampled soil and vegetation are displayed in Fig. 1 and Figs. 1, 2, and 3 of Online Resource 1. The average mean annual precipitation (MAP) for the study plots was 802 mm yr^{-1}, ranging from 510 mm yr^{-1} to 1363 mm yr^{-1}, whereas the average mean annual temperature (MAT) was 23.8 °C, ranging from 20.5 °C to 26.8 °C. The study plots had an average elevation of 535 m asl, varying from 99 to 944 m asl (Table 1). Vegetation structure ranged from open canopies 4–7 m in height to closed canopies 25–30 m tall. Study sites consist of well-conserved structurally mature stands, though sporadic grazing and occasional timber logging cannot be fully disregarded in a few study plots. Most plots were established on flat terrain, with some on slightly sloping reliefs. A more detailed version of Table 1 with environmental and vegetation data is available in Table 1 of Online Resource 1. Vegetation inventory and soil sampling were conducted during three fieldwork campaigns in 2017, 2018, and 2019, as part of the inventory carried out by the *Nordeste Project fieldwork team*. In all years, sampling was consistently carried out during the late wet season to capture vegetation at its maximum vegetation development stage (Moonlight et al. 2021).

Table 1: Study plots, selected environmental and vegetation data: plot code; latitude; longitude; APS = average plot slope; F = flat; SS = slightly sloping; geology; SED = sedimentary; CRY = crystalline; CAR = carbonate; RSG = reference soil group; MAP = mean annual precipitation; MAT = mean annual temperature; elevation; AGB_W = above-ground woody biomass; clay (fraction); $[N]_T$ = soil total nitrogen; $[P]_T$ = soil total phosphorus; pH_{H2O} = water-measured soil pH; $[Ca]_{ex}$ = soil exchangeable calcium. Study plots are ordered according to increasing MAP. Soil data refers to the upper 0.3 m from the soil surface. Original vegetation and soil data are integrated into the *ForestPlots Network* (www.ForestPlots.net).

Plot Code	Latitude	Longitude	APS	Geology	RSG	MAP (mm)	MAT (C°)	Elevation (m)	AGB_W (Mg ha^{-1})	Clay (fraction)	$[N]_T$ (mg g^{-1})	$[P]_T$ (mg kg^{-1})	pH_{H2O}	$[Ca]_{ex}$ ($mmol_c$ kg^{-1})
CND-01	-9.97	-39.01	F	SED	Arenosol	512	22.7	535	20.9	0.04	2.5	69	4.66	1.5
GBR-02	-11.02	-41.41	F	CAR	Leptosol	515	22.9	637	47.3	0.15	16.8	1194	7.48	55.8
GBR-01	-11.01	-41.44	F	CAR	Cambisol	519	23.3	564	74.8	0.22	12	469	7.77	55.7
LGE-01	-9.05	-40.32	F	CRY	Luvisol	591	25.1	390	10.2	0.12	11.9	148	5.47	17.4
MOR-02	-11.50	-41.35	SS	SED	Leptosol	591	20.8	907	15.8	0.16	19	223	4.17	3.4
CGR-01	-7.28	-35.98	F	CRY	Luvisol	599	22.8	487	14.1	0.18	8.8	162	4.71	8.6
MOR-01	-11.49	-41.33	F	SED	Arenosol	602	20.5	944	18.8	0.06	16.8	51	4.49	7.7
IBD-02	-10.79	-42.78	F	SED	Arenosol	684	25.6	411	19.7	0.02	3.3	92	5.68	3.3
IBD-01	-10.79	-42.82	SS	SED	Arenosol	696	25.5	421	18.5	0.01	6.1	61	5.74	5.9
BVT-01	-12.73	-40.71	SS	CRY	Acrisol	724	22.2	495	22.5	0.24	12.1	52	4.32	4.6
SET-01	-7.97	-38.38	F	CRY	Luvisol	752	23.7	472	27.8	0.08	6.3	144	6.13	30.8
SCP-02	-8.86	-42.68	F	SED	Acrisol	768	25.6	487	20.6	0.15	20.5	89	4.3	0.9
MCS-02	-13.06	-42.52	F	CRY	Arenosol	782	24.4	545	33.9	0.06	5.1	43	5.67	12.3
SCP-01	-8.86	-42.70	F	SED	Cambisol	786	25.4	529	11.7	0.21	7.1	302	4.27	2.5
MCS-01	-13.00	-42.71	SS	CRY	Leptosol	789	23.1	770	46.9	0.12	13.4	103	4.54	2.9
PAT-01	-7.01	-37.40	F	CRY	Luvisol	792	26.2	282	18.3	0.18	10.1	204	5.86	25.9
SJO-01	-8.81	-36.41	F	CRY	Arenosol	792	21.4	670	12.7	0.06	6.6	164	5.15	5.3
PAT-02	-7.02	-37.40	F	CRY	Luvisol	808	26.2	283	21.2	0.15	5.9	163	6.27	25.1
SDA-03	-5.12	-40.87	F	CRY	Luvisol	815	25.5	309	55.6	0.11	9.5	163	5.97	30
CJU-01	-14.97	-43.92	F	SED	Arenosol	825	24.2	470	4.9	0.07	6.7	15	4.77	2.5
PFF-01	-5.04	-37.52	F	CAR	Calcisol	864	26.8	99	33.6	0.42	20	360	7.89	65.6
JUV-01	-14.43	-44.16	SS	SED	Luvisol	900	24.2	518	85.7	0.28	11.4	176	6.14	27.4
CTI-01	-14.22	-42.53	SS	CRY	Regosol	939	20.9	938	60.9	0.15	10.7	28	4.38	3.6
SDA-02	-5.14	-40.91	F	SED	Leptosol	969	23.3	640	48.7	0.22	13.2	181	4.21	0.4

SDA-01	-5.15	-40.93	F	SED	Arenosol	973	23	682	22.2	0.07	12.1	129	4.51	0.8
ARI-04	-7.36	-39.48	F	SED	Acrisol	1011	21.4	899	10.6	0.29	15	101	4.47	1.8
ARI-03	-7.27	-39.45	SS	SED	Alisol	1081	22	796	83.2	0.12	9.5	80	4.22	4.3
BTI-01	-3.36	-41.74	SS	SED	Leptosol	1222	26.6	102	46	0.17	28.9	282	4.65	17.2
PSC-02	-4.13	-41.68	F	SED	Regosol	1363	26	238	37	0.09	7.8	156	4.58	0.9

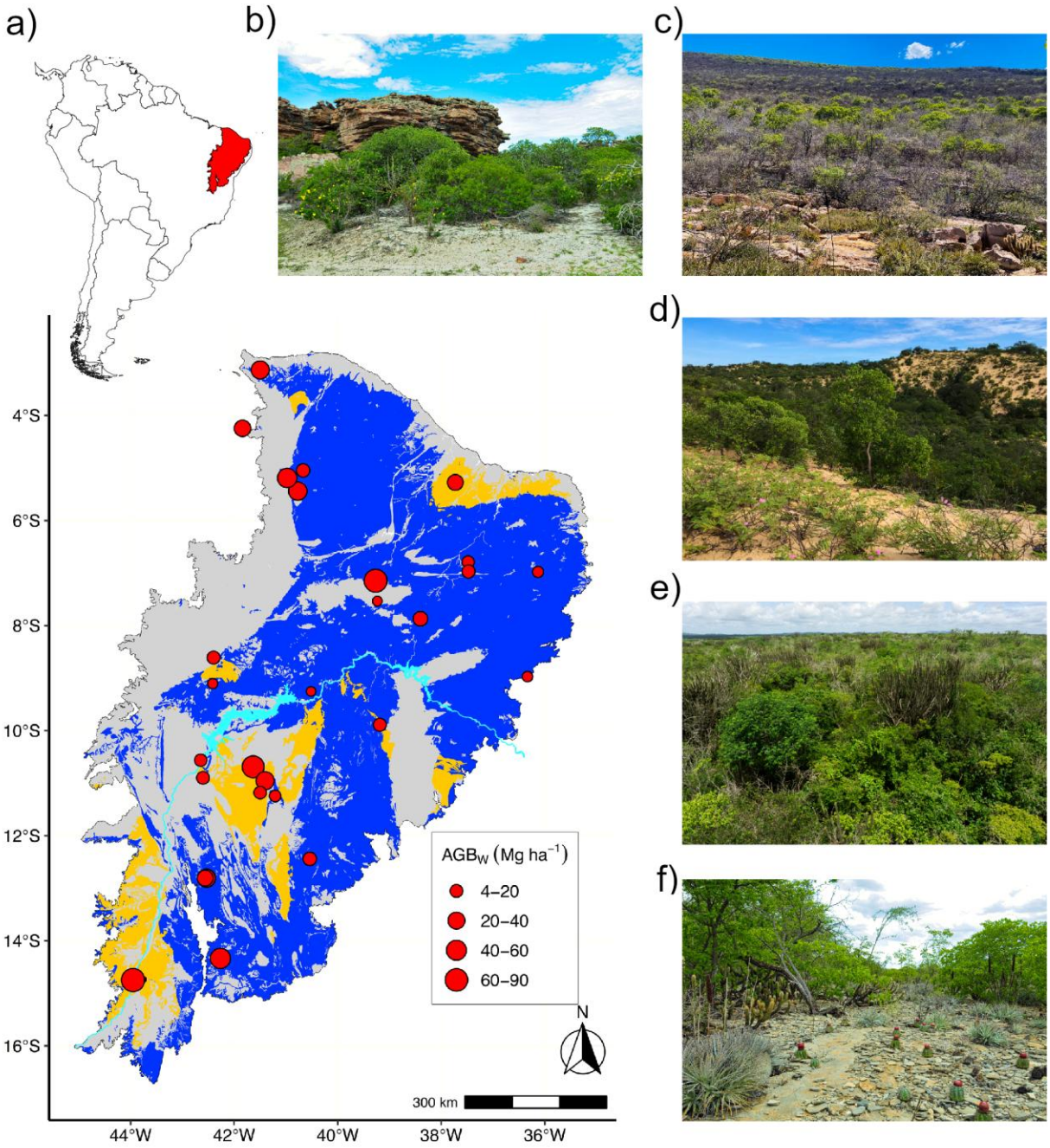

Fig. 1: Study plots and sampled vegetation. a) Geographic location of the Brazilian Caatinga region in South America and the distribution of dry above-ground woody biomass (AGB_W) across the *Nordeste Project* study plots. b) Caatinga *sensu stricto* interspersed with exposed sand in the sedimentary Morro do Chapéu Formation (MOR-01); c) Caatinga *sensu stricto* interspersed with arenites outcrops in the sedimentary Morro do Chapéu Formation (MOR-02); d) Caatinga *sensu stricto* in the Quaternary dunes of the middle São Francisco River (IBD-01); e) Caatinga *sensu stricto* in the crystalline São Caetano Formation (CGR-01); f) Caatinga *sensu stricto* overlying carbonate rock outcrops in Gruta dos Brejões (GBR-02). Blue, grey, and yellow areas indicate crystalline, sedimentary, and carbonate substrates, respectively. The light blue course depicts the *São Francisco* River. The outline of the Caatinga region follows the Brazilian Institute of Geography and Statistics (IBGE, 2019), crystalline and sedimentary substrates according to the geoscience system of the Geological Survey of Brazil (CPRM), and areas with carbonate substrates according to Queiroz et al. (2017). Overlapping study plots have been displaced to allow their visualisation. Datum: SIRGAS2000. Photos by Domingos Cardoso (b, c, d, and f) and Peter Moonlight (e).

Vegetation structure

Standardised floristic and structural inventories were carried out following '*The DryFlor Field Manual for Plot Establishment and Remeasurement*' (Moonlight et al. 2021a; 2021b). In brief, a 100 × 50 m (0.5 ha) plot was established and sub-partitioned into 50 subplots (10 × 10 m or 0.01 ha). All trees with stems with ≥ 5 cm in diameter were inventoried, measured at both breast height (DBH, 1.3 m from the ground) and 30 cm from the ground level (DGL), as recommended by the DRYFLOR protocol to ensure comparability across dry forest networks. This criterion represents a compromise that balances practical field constraints with the need to capture most of the forest's structure and dynamics. Multi-stemmed individuals were carefully measured stem by stem. Trees were identified in the field, herbarium, and by taxonomic specialists, to species where possible, and voucher specimens were deposited into the Herbarium of Feira de Santana State University (HUEFS; Feira de Santana, Bahia, Brazil). Tree-by-tree data from each '*Nordeste Project'* study plot contribute to the *ForestPlots network* (ForestPlots.net, 2021) and are curated at www.ForestPlots.net. High-resolution images of the voucher specimens are also publicly accessible through the *species*Link network of biodiversity collections (http://www.splink.org.br/).

Soil sampling

We used a standard protocol (https://rainfor.org/wp-content/uploads/sites/129/2022/07/soilandfoliarsampling.pdf) with some adjustments to accommodate specific characteristics of Caatinga soils, such as restricted depth range, and a marked presence of stones and rocks in some cases. This protocol has been widely used in past research conducted in tropical regions, such as the RAINFOR and TROBIT networks (e.g., Quesada et al., 2010; Lloyd et al., 2015). Specifically, four auger cores were taken as baseline samples in each plot, with one to three additional cores collected in cases of pronounced spatial variability within the plot (e.g., irregular topography, rock outcrops, vegetation changes, or markedly shallow soils). Samples were obtained at standard depth intervals (0–5, 5–10, 10–20, 20–30, 30–50, 50–100, 100–150, and 150–200) or according to the maximum depth achievable at each location. In addition, a soil pit was excavated just beside each plot to describe soil profiles, also serving as an additional sampling point for chemical and physical analyses. Subsequently, all samples were air-dried and sent to the Soil and Plant

Thematic Laboratory at the National Institute for Research in the Amazon (LTSP, INPA, Manaus, Amazonas, Brazil).

Laboratory analysis

In the LTSP, samples were loosened, sieved with a no. 10-mesh sieve (particle size of 2 mm), and any non-fine earth residues removed (e.g., gravels and vegetation or faunal debris). We determined water-measured soil pH (pH_{H2O}) using a 1: 2.5 soil-to-deionised water ratio with a glass electrode. Soil exchangeable cations were determined by the Silver-Tioureia (AgTU) method (Pleysier and Juo 1980). The concentration of each cation extracted was determined using an Atomic Absorption Spectrophotometer (AAS, Model 100b, Perkin Elmer, Norwalk, CT, USA). Soil sum of bases ($\sum_B$) and effective cation exchange capacity (I_E) were calculated according to Eqn. (1) and (2), respectively:

$$\sum_B = [Ca]_{ex} + [Mg]_{ex} + [K]_{ex} + [Na]_{ex} \quad \text{Eqn. (1)}$$

$$I_E = \sum_B + [Al]_{ex} \quad \text{Eqn. (2)}$$

Where Ca, Mg, K, Na and Al refer to calcium, magnesium, potassium, sodium and aluminium, respectively, while "ex" refers to exchangeable contents.

Soil total carbon (C) and nitrogen (N) were determined using dry combustion with an automated analyser (Vario Max CN, Elementar, Germany). Soil samples were combusted at high temperatures, and the resulting gases were measured to quantify C and N concentrations. Soil total phosphorus concentrations, $[P]_T$, were obtained using composite samples from the 0–5, 5–10, 10–20, and 20–30 cm soil depths. Samples were digested with concentrated sulfuric acid, followed by the addition of hydrogen peroxide (Tiessen and Moir 1993). Afterwards, $[P]_T$ were determined by colourimetry using the molybdenum blue colour development method (Olsen and Sommers 1982), using a spectrophotometer (Model 1240, Shimadzu, Kyoto, Japan). Soil texture was determined using the sieve-pipette method (Gee and Bauder 1986). Soil dry bulk density (BD) was determined using the volumetric ring method (Eijkelkamp Agrisearch Equipment BV, Giesbeek, Netherlands). Calibration procedures and standard samples were routinely used to ensure the accuracy of the results.

Soil classification, clay mineralogy, and geological surveying

The soils were classified according to the World Reference Base for Soil Resources (IUSS Working Group WRB, 2014/2015), with the aid of the WRB Tool 1.1.2.0 (Downloaded in March 2021; OrlovDO, 2017; https://apps.microsoft.com/store/detail/wrb-tool/). This tool streamlines the soil classification process by guiding users systematically through the key steps, potentially reducing classification errors through its step-by-step interface. Complete soil classifications are provided in Table 2 of Online Resource 1. Following Quesada et al. (2020), we categorised the sampled soils as HAC, LAC, and 'Arenic'. HAC soils are those with CEC $clay^{-1}$ > 24 $mmol_c\ kg^{-1}$ (typically less weathered soil classes such as Luvisols in this study), while LAC soils are those with CEC $clay^{-1}$ < 24 $mmol_c\ kg^{-1}$ (typically more weathered soils such as Acrisols, Alisols, and Regosols in this study) (IUSS Working Group WRB, 2014/2015). The third category ('Arenic') was used for considerably sandy soils, i.e., those soils with loamy sand texture or coarser (Arenosols in this study). Additionally, we used the geoscience system (GeoSGB; https://geosgb.sgb.gov.br/geosgb/) of the Geological Survey of Brazil (CPRM), and the delineation of areas with carbonate rocks as in Queiroz et al. (2017) to characterise the geology of each study plot.

Maximum plant-available soil water (θ_P)

The maximum plant-available soil water (θ_P) is defined as the difference in volumetric soil water content (θ_v) values between field capacity (θ_v at a matric potential of -10 kPa: $\theta_{v,FC}$) and the permanent wilting point (θ_v at a matric potential of -1500 kPa: $\theta_{v,WP}$): $\theta_{v,FC}$ - $\theta_{v,WP}$. These θ_v values can be obtained from the water retention curve (WRC), which for our study was described with the widely used van Genuchten (VG) equation (van Genuchten, 1980). The VG parameters required for the calculation of the WRC were obtained from Table 6 in Hodnett and Tomasella (2002). These parameters had been obtained using a (soil) class pedotransfer function approach for tropical soils of the IGBP soils dataset. For each *Nordeste* plot, and each soil layer, the soil textural class, based on measured sand/silt/clay contents, was determined using the USDA soil texture triangle, after which the look-up table provided by Hodnett and Tomasella (2002) was used to obtain the VG parameters. After estimating $\theta_{v,FC}$ and $\theta_{v,WP}$ from the constructed WRCs, their difference was integrated over the maximum measured soil depth (mm), thus providing θ_P in $mm^3\ mm^{-2}$, or simply mm.

246 Climatic data

247 Climatic data were extracted from the WorldClim database version 2.1. The BioClim variables
248 represent the historical averages for the 1970 – 2000 period with 30 arc-seconds (~1 km²) resolution (Fick and
249 Hijmans 2017). We selected a few key variables based on *a priori* hypotheses, i.e., mean annual precipitation
250 (BIO12 in the WorldClim system, MAP in this study), mean annual temperature (BIO1 in the WorldClim
251 system, MAT in this study), the maximum temperature of the warmest month (BIO5 in the WorldClim system,
252 T_{MAX} in this study), and precipitation seasonality (BIO15 in the WorldClim system, Ψ in this study). T_{MAX}
253 reflects high-temperature events throughout the year and can be used to examine whether vegetation properties
254 are affected by extreme temperature events, while BIO15 is a measure of variation in monthly precipitation
255 totals over the year (O'Donnell and Ignizio 2012). Potential evapotranspiration (PET) was obtained from the
256 CGIAR Consortium for Spatial Information ─ CGIAR-CSI (Zomer et al., 2022). Estimates of climatic water
257 deficit (CWD) for each study plot were obtained from raster layers (currently available at
258 https://zenodo.org/records/14932971) with 2.5 arc-minute resolution. The CWD variable was found to be
259 important in determining allometric relationships (Chave et al. 2014) and represents the net balance between
260 precipitation and potential evapotranspiration (PET) in the dry months (i.e., months where PET exceeds rainfall,
261 given in mm per year). Note that although CWD values are originally negative, we present them as positive to
262 indicate 'millimetres of deficit'.

263

264 Above-ground woody biomass (AGB_W) calculations

265 Estimates of AGB_W for individual tree stems were calculated using an allometric equation specifically
266 developed for Caatinga trees (Sampaio and Silva 2005):

267 $$AGB_T = 0.0644 \times DGL^{2.3948} \quad \text{Eqn. (3)}$$

268 Where AGB_T is the dry tree above-ground biomass (kg) and DGL is the diameter at the ground level.
269 Biomass of individual cacti (1,098 stems) was estimated using a separate specific equation for cacti from
270 Sampaio and Silva (2005), and palm tree biomass (35 stems) was calculated using a formula from Saldarriaga
271 et al. (1988). At the plot level, total AGB_W was the sum of the above-ground dry biomass of all stems measured,

with individual biomass for multi-stemmed individuals calculated and then summed. It is worth noting that the equation determines the total biomass of trees (including leaves), with "w" referring to woody species.

Community functional composition

Following Prado-Junior et al. (2016), we calculated two community-weighted trait means of strong ecological significance: community-weighted maximum stem diameter (CWM_{DMAX}) and community-weighted mean wood density (CWM_{WD}). Both traits represent fundamental life history strategies and are closely linked to resource storage, structural resistance, hydraulic safety, and the ability to adapt to environmental stressors (Larjavaara and Muller-Landau 2010; Reich 2014). Species maximum stem diameter reflects adult sizes and was calculated as the upper 0.95 percentile of those trees with a stem diameter $\geq 0.1 \times$ the diameter (cm) of the thickest tree observed in each population. We adopted this approach since it was considered the least sensitive to varying sample sizes while providing robust estimates for both larger and smaller species (King et al. 2006; Prado-Junior et al. 2016). Species' wood density values were extracted from the global wood density database (Chave et al. 2009; Zanne et al. 2009). When unavailable at the species level, we used wood density values at the genus or family levels. Botanical names were checked and adjusted according to the *Flora do Brasil* 2020 with the *flora* package version 0.3.5 (Carvalho 2020). Each trait was weighted according to the basal area of individual species, as this is expected to reflect plant performance better than abundance (Prado-Junior et al. 2016). The distribution of a given trait across a niche space can be summarised along orthogonal axes, from which functional diversity indices can be calculated (Mason et al. 2005). Specifically, we derived the functional richness index (F_{RIC}) from community-weighted maximum stem diameter and wood density, measuring the amount of functional trait space occupied by a community. The functional richness index reflects the diversity of ecological strategies present and is calculated as the convex hull volume in a multidimensional trait space. Community-weighted mean traits and F_{RIC} were computed using the FD package in R (Laliberté et al. 2014).

Data analysis

Initially, AGB_W values were plotted against three categorical predictors: geological substrates, clay activity, and RSGs. To assess whether these categories explained variations in AGB_W, a robust non-parametric

Kruskal-Wallis test (χ^2) was performed. Comparisons were limited to categories with at least 5 observations, including Arenosols, Leptosols, and Luvisols for RSGs; HAC, LAC and Arenic for clay activity; and crystalline (S_{CRY}) *versus* sedimentary (S_{SED}) for geological substrates.

To test the hypothesis that AGB_W is influenced by multiple environmental factors and their interactions, a linear mixed-effects model was employed, combined with multi-model/model averaging inferences. For this purpose, two 0.25 ha subplots were considered within each 0.5 ha plot (29 total), resulting in 58 observations. This procedure was adopted to increase the number of observations and to provide greater flexibility for including multiple predictors in the same models, while reducing the risk of overfitting (Harrison et al. 2018). The global model included mean annual precipitation and climatic water deficit to represent water input and water balance, and maximum temperature of the warmest month as a key thermal variable. Correlations between climatological variables are provided in Table 3 of Online Resource 1.

Since soil predictors were strongly correlated (Table 4, Online Resource 1), they were carefully selected by systematically replacing them one at a time in the global model (Eqn. 4). We evaluated relative importance values (RIV), variance inflation factors (VIF), marginal r^2 (fixed effects), and Akaike Information Criterion corrected (AICc). The VIF values of all predictors in Eqn. (4) were checked to prevent overfitting. Given the high correlation between potential evapotranspiration and temperature variables ($\rho = 0.84$, $p < 0.001$ for MAT; and $\rho = 0.83$, $p < 0.001$ for T_{MAX}, Table 3 of Online Resource 1), and considering that PET was incorporated into CWD, we did not include it in the global model of Eqn (4). In all analyses, we used the upper 0-30 cm soil layer, commonly used in vegetation ecology studies (e.g., Quesada et al. 2012; Lloyd et al. 2015). To facilitate interpretation, all predictors were standardised (subtracting the mean and dividing by the standard deviation) with the aid of the *caret* package in R (Max et al. 2020), providing comparative effect sizes among predictors. Since the analysis involved non-independent observations, sites were treated as random structures within the model (Harrison et al. 2018). The final global model is expressed by Eqn. (4):

$$\log(\mathrm{AGB_w}) = \beta_0 + \beta_1\theta_\mathrm{P} + \beta_2\mathrm{MAP} + \beta_3[\mathrm{Ca}]_\mathrm{ex} + \beta_4\mathrm{CWD} + \beta_5\theta_\mathrm{P} \times \mathrm{CWD} + \beta_6[\mathrm{Ca}]_\mathrm{ex} \times \mathrm{CWD} + \beta_7 T_\mathrm{MAX} + \beta_8\log[\mathrm{N}]_\mathrm{T} + \beta_9\log[\mathrm{P}]_\mathrm{T} + (1|\mathrm{site}) + \varepsilon \quad \text{Eqn. (4)}$$

Where AGBw is above-ground woody biomass; θ_P is maximum plant-available soil water; MAP is mean annual precipitation; $[Ca]_{ex}$ is soil exchangeable calcium; CWD is climatic water deficit; T_{MAX} is the

maximum temperature of the warmest month; $[N]_T$ is soil total nitrogen; $[P]_T$ is soil total phosphorus; (1|site) represents the random intercept for site; and ε is the residual error. We evaluated the distribution of residuals both statistically and graphically. The response variable was log-transformed to meet the normality assumption and reduce heteroscedasticity. The potential presence of spatial structures was checked using the methods outlined by Bauman et al. (2018a; 2018b). Specifically, the *listw.candidates* function from the *adespatial* package in R (Dray et al. 2021) was used to test a few distance and graph-based spatial weighting matrices. Spatial autocorrelations were assessed through Moran's *I* coefficient with a significance level of $p \leq 0.05$.

We tested all possible predictor combinations using the *MuMIn* package in R (Bartón 2020). Collinearity issues were further controlled by preventing predictors with Pearson's correlation $|r| \geq 0.6$ in the same models. This process generated 137 unique models, with the maximum number of predictors in each model being constrained to 6, thus ensuring nearly 10 observations per model term. Model selection followed an information-theoretic (I-T) approach, retaining models with ΔAICc < 4 (Burnham et al. 2011; Harrison et al. 2018). From the 19 retained models (ΔAICc < 4), coefficients were averaged using the *model.avg* function of the *MuMin* R package. Full averaging was used for model predictions, providing more reliable β estimates when multiple models have support (Mazerolle 2023). The 'full' averaging approach dictates that each variable is included in every model (setting the coefficients to zero in the models where the term is absent), whereas the 'conditional' average approach considers only those models where the parameter appears (Bartón 2020). In both cases, average coefficients were weighed according to Akaike weights. Model marginal r^2 (r^2m) was reported to represent fixed effects. Additionally, we performed a series of 95th-percentile linear mixed-effects model relationships to explore the predictive ability of individual soil and climate predictors on AGB_W.

A Spearman's rank correlation matrix (ρ) was computed to explore relationships between soil properties and community functional properties, with significant relationships graphically represented (Fig. 7 of Online Resource 1). Subsequently, the most supported variables identified through the multi-model inference approach were used to investigate the relationships between environmental factors, vegetation properties, and their combined effects on AGB_W. For this task, we employed a Structural Equation Modelling (SEM) framework using the *lavaan* R package (Rosseel 2012). The model assessed direct and indirect effects of edaphic and climatic variables, i.e., mean annual precipitation, climatic water deficit, soil exchangeable

calcium, and maximum plant-available soil water on community-weighted maximum stem diameter, wood density, and associated functional richness, as well as their potential effects on above-ground biomass (AGB_W).

To overcome the non-normality of some variables included in the SEM, we utilised the Maximum Likelihood Estimator with Robust Standard Errors (MLR), which adjusts for non-normal distributions and potential heteroscedasticity. Robustness was further enhanced with the *Yuan-Bentler* scaling correction, which is appropriate for handling non-normality and small sample sizes. The SEM was evaluated using multiple fit indices, including the Comparative Fit Index (CFI), Tucker-Lewis Index (TLI), Root Mean Square Error of Approximation (RMSEA), and Standardised Root Mean Square Residual (SRMR), with robust versions addressing non-normality. Overall model performance was assessed using the chi-square test statistic (χ^2) and its associated *p-values* to determine significance.

Finally, we used the *alphahull* R package (Pateiro-Lópes and Rodríguez-Casal 2019) to make the heatmaps presented in Figs. 3 and 4. We used heatmaps to represent interaction terms, as they provide an intuitive visualisation of how AGB_W responds across the gradients of two predictors simultaneously. Heatmap simulations were constrained to the actual environmental conditions found in the dataset. All graphs were created using the *ggplot2* R package (Wickham et al. 2016), and all analyses were conducted in the R environment, Version 4.1.1 (R Core Team 2021).

Results

Stand structure and categorical predictors

Altogether, 18,201 individual stems with a diameter at the ground level ≥ 5 cm were recorded across the 29 study plots, including 1,098 cacti and 35 palm trees. These individuals encompass 331 unique species, 176 genera, and 50 identified tree families. The mean ± standard deviation of AGB_W was 32.55 ± 22.35 Mg ha^{-1} (min = 4.87 Mg ha^{-1}; max of 85.65 Mg ha^{-1}), mean stem density (stems ha^{-1}) was 1255 ± 489 (min = 492; max = 2,534), and mean basal area (B_A) was 12.89 ± 7.10 m^2 ha^{-1} (min = 2.44; max = 28.79 m^2 ha^{-1}). Above-ground woody biomass did not differ among geological substrates ($\chi^2 = 0.08$; $p = 0.775$; Fig. 4-a of Online Resource 1), types of clay activity ($\chi^2 = 3.70$; $p = 0.157$; Fig. 4-b of Online Resource 1), and RSGs ($\chi^2 = 3.39$; $p = 0.183$; Fig. 4-c of Online Resource 1).

Above-ground woody biomass modelling

Above-ground woody biomass was influenced by both edaphic and climatic factors, and their interactions, as indicated by the multi-model Inference and Information-Theoretic approaches. Of the 19 models selected within the ΔAICc < 4 range, six included climate, soil chemistry, and soil physics terms; 10 included only climate and soil chemistry; and three included only soil chemistry (Table 5 of Online Resource 1). The most strongly supported terms in the conditional average model were the interaction between exchangeable calcium and climatic water deficit (β = -0.43), exchangeable calcium (β = 0.40), mean annual precipitation (β = 0.28), and the interaction between maximum plant-available soil water × climatic water deficit (β = -0.25) (Fig. 2-A). Relative importance values for these terms were: exchangeable calcium (0.95), mean annual precipitation (0.92), climatic water deficit (0.53), the interaction between exchangeable calcium and climatic water deficit (0.40), maximum plant-available soil water (0.33), max temperature of the warmest month (0.18), the interaction between maximum plant-available soil water × climatic water deficit (0.18), total nitrogen (0.15), and total phosphorus (0.02) (Fig. 2-b).

Replacing collinear soil predictors in the global model (Eqn. 4) showed that r^2m decreased in the following order: exchangeable calcium (0.49) > sum of bases (0.48) > effective cation exchange capacity (0.46) > pH_{H2O} (0.45) > exchangeable magnesium (0.41) > exchangeable aluminium (0.40) > exchangeable sodium (0.39) > exchangeable potassium (0.35). Correspondingly, AICc values increased, with exchangeable calcium showing the lowest (92.95) and exchangeable potassium the highest (100.78). RIV decreased in the order: effective cation exchange capacity (0.96) > exchangeable calcium (0.95) > sum of bases (0.87) > pH_{H2O} (0.64) > exchangeable magnesium (0.46) > exchangeable sodium (0.39) > exchangeable potassium (0.31) > exchangeable aluminium (0.15). Based on these metrics, and noting the dominance of exchangeable calcium in the soil cation exchange complex across most sites (Fig. 5 of Online Resource 1), exchangeable calcium was selected over its alternatives. Model-simulated responses suggest that exchangeable calcium levels have a marked influence on AGB_W. This effect, however, was also influenced by the intensity of the climatic water deficit (Fig. 3-a).

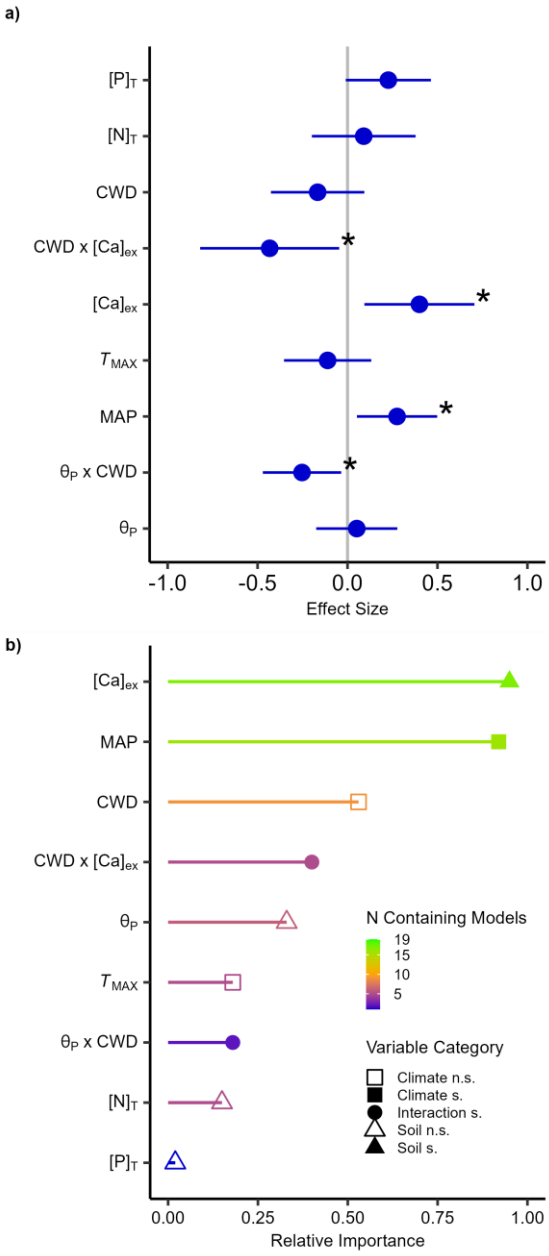

Fig. 2: Multi-model inference statistics. a) edaphic and climatic effects on above-ground woody biomass (AGB_W) of 29 Caatinga's SDTFs study plots. Points represent conditional average model coefficients. Coefficients were standardised, thus representing changes in $\log(AGB_W)$ for a one standard deviation change in the predictor variable (effect size). $[Ca]_{ex}$ = exchangeable calcium; MAP = mean annual precipitation; CWD = climatic water deficit; θ_P = maximum plant-available soil water; T_{MAX} = temperature of the warmest month; $[N]_T$ = soil total nitrogen; $[P]_T$ = soil total phosphorus. Error bars show 95% confidence intervals. Asterisks denote statistically significant coefficients. b) Relative importance values (RIV) of each variable included in the final model. Variable category and the frequency of each term across the 19 models selected via AICc ("N Containing Models") are shown. Filled symbols represent significant relationships, while empty symbols represent non-significant relationships.

Using coefficients from the best AICc-ranked model (Model 1; Table 5 of Online Resource 1), predicted above-ground woody biomass ($\hat{AGB}_W$) was virtually constant across climatic water deficit when exchangeable calcium was low (~5 $mmol_c\ kg^{-1}$). However, at high exchangeable calcium (~40.37 $mmol_c\ kg^{-1}$), $\hat{AGB}_W$ ranged from 19.19 to 86.12 Mg ha^{-1} as climatic water deficit varied from 1238 to 909 mm. Similarly, model predictions showed that $\hat{AGB}_W$ increases with higher maximum plant-available soil water and lower

climatic water deficit (Fig. 3-b). For instance, at a maximum plant-available soil water = 200 mm, $A\hat{G}B_W$ was 62.15 Mg ha^{-1} when climatic water deficit was low (620 mm), but dropped to 14.30 Mg ha^{-1} at high climatic water deficit (1290 mm). The second-best model (Model 2; Table 5 of Online Resource 1) highlighted the influence of mean annual precipitation and exchangeable calcium on $A\hat{G}B_W$. For example, at a mean annual precipitation of ~800 mm, $A\hat{G}B_W$ varied from 20.14 to 60.81 Mg ha^{-1} as exchangeable calcium increased from 1.37 to 62.87 $mmol_c\ kg^{-1}$ (Fig. 3-c).

Finally, $A\hat{G}B_W$ predictions across the mean annual precipitation gradient in the dataset were simulated under varying soil conditions (Fig. 4): A) optimal − exchangeable calcium = 50.67 $mmol_c\ kg^{-1}$, and maximum plant-available soil water = 270 mm; B) moderately high − exchangeable calcium = 32.65 mmolc kg^{-}, and maximum plant-available soil water = 210 mm; C) intermediate − exchangeable calcium = 14.62 $mmol_c\ kg^{-1}$, and maximum plant-available soil water = 150 mm; and D) poor conditions − exchangeable calcium = 1 $mmol_c\ kg^{-1}$, and maximum plant-available soil water = 80 mm. While $A\hat{G}B_W$ increased with mean annual precipitation in all cases, this effect was strongest under favourable soil conditions, i.e., increased nutrient content and higher water storage capability.

434

435

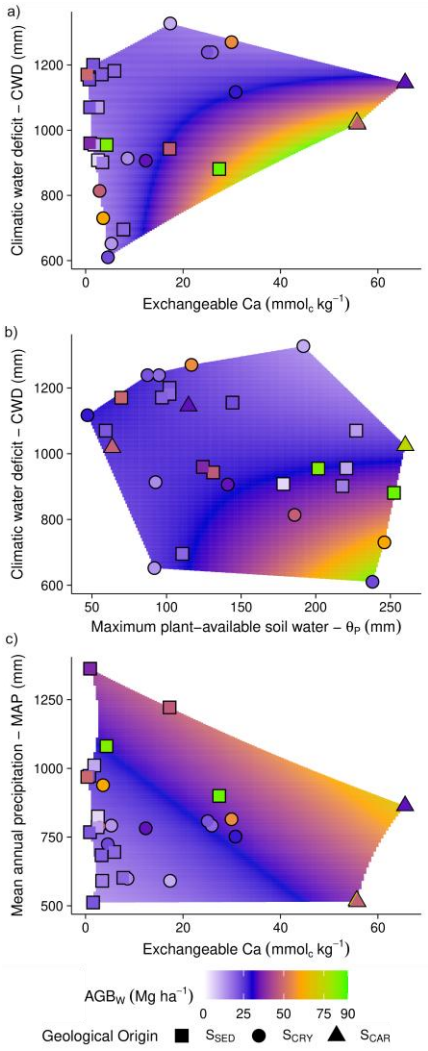

Fig. 3: Modelled responses of above-ground woody biomass ($A\hat{G}B_W$) based on the two best AICc-ranked models. a) AGB_W as a function of the interaction between exchangeable calcium ($[Ca]_{ex}$) and climatic water deficit (CWD). b) AGB_W as a function of the interaction between CWD and maximum plant-available soil water (θ_P). c) AGB_W as an additive function of $[Ca]_{ex}$ and mean annual precipitation (MAP). Study plots are shown within their respective environmental domains and geological categories. Note: CWD, originally expressed as negative values, is presented here as positive values representing "millimetres of deficit." Geological categories: SED = sedimentary, CRY = crystalline, CAR = carbonate.

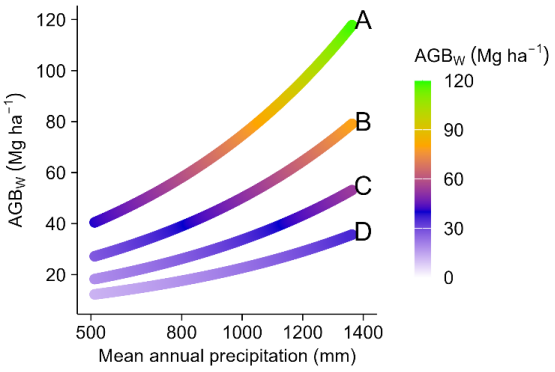

Fig. 4: Modelled responses of above-ground woody biomass as ($A\hat{G}B_W$) a function mean annual precipitation under four edaphic scenarios: A) optimal – maximum plant-available soil water (θ_P) and exchangeable calcium ($[Ca]_{ex}$) (+2 SD above the mean); B) moderately high – θ_P and $[Ca]_{ex}$ (+1 SD above the mean); C) intermediate – θ_P and $[Ca]_{ex}$ (at their means); and D) poor conditions – θ_P and $[Ca]_{ex}$ (–1 SD below their means).

Regarding bivariate relationships, we found significant associations between AGB_W and soil variables, including exchangeable calcium, sum of bases, effective cation exchange capacity, sand, and silt, across the full dataset, while climatic variables showed no significant linear relationships with AGB_W (Table 6 of Online Resource 1 and Fig. 6 of Online Resource 1).

Associations between soil properties and community functional composition

A Spearman's correlation matrix showed that community-weighted wood density was inversely correlated with several soil properties, including exchangeable calcium, sum of bases, effective cation exchange capacity, and silt content, and positively correlated with soil sand. Conversely, community-weighted maximum stem diameter was positively associated with exchangeable calcium and soil sum of bases. The functional richness index was positively correlated with multiple soil properties, including exchangeable Ca, Mg, K, sum of bases, and effective cation exchange capacity. Significant Spearman's coefficients are shown in Fig. 7 of Online Resource 1, and all tested relationships are summarised in Table 7 of Online Resource 1. No significant correlations were found between climatic variables and functional properties. Finally, forests in crystalline environments had higher functional richness values than those in sedimentary substrates ($\chi^2 = 7.71$; $p = 0.005$; Fig. 8-c of Online Resource 1), while community-weighted mean wood density and maximum stem diameter did not differ significantly among these categories, though forests in the carbonate category showed a tendency for lower community-weighted wood density and higher stem diameters values.

Structural Equation Modelling (SEM)

Among the metrics utilised to evaluate our SEM (Fig. 5), the Robust Comparative Fit Index (CFI) was 0.992 (standard) and 0.989 (robust), suggesting an excellent fit. The Tucker-Lewis Index (TLI) values were 0.917 (standard) and 0.884 (robust), indicating a good overall model fit. The Root Mean Square Error of Approximation (RMSEA) was 0.076 (standard) and 0.092 (robust), both within acceptable thresholds for good fit (Browne and Cudeck 1992). The Standardised Root Mean Square Residual (SRMR) was 0.063, indicating a good fit for the data. Although this statistic can be sensitive to sample size, the *Chi-square* was 2.339 (standard) and 2.552 (scaled), with a *p-value* of 0.282, indicating an acceptable model fit. Noting that, except for AGB_W,

all variables were standardised, significant relationships included the negative effect of exchangeable soil calcium on community-weighted mean wood density (β = -0.59, p < 0.001), its positive impact on community-weighted mean maximum stem diameter (β = 0.42, p = 0.031), and its marginal effect on functional richness (β = 0.24, p = 0.093). Above-ground biomass (AGB_W) was significantly influenced by community-weighted mean maximum stem diameter (β = 10.17, p < 0.001), mean annual precipitation (β = 7.89, p = 0.001), and soil available calcium (β = 9.27, p = 0.012) (Fig. 5).

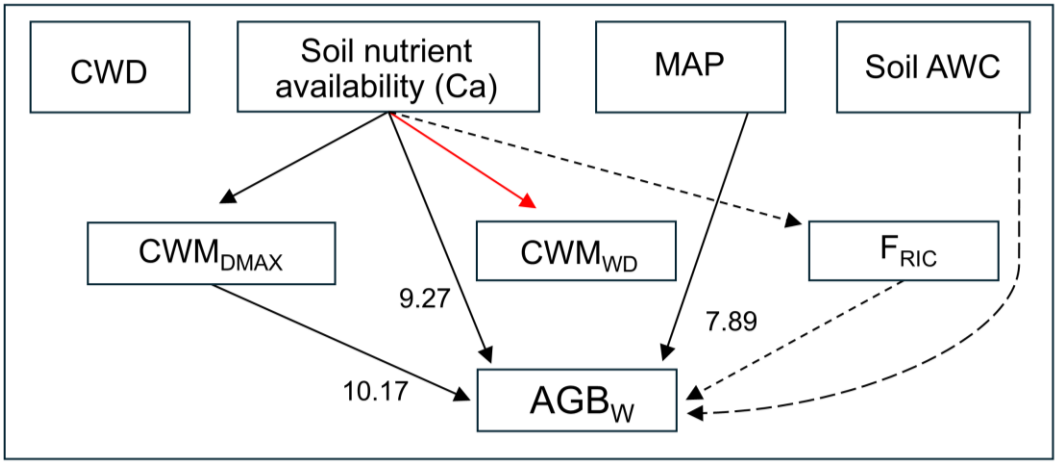

Fig. 5: Structural equation model (SEM) showing the relationships between environmental variables [climatic water deficit (CWD), soil nutrient availability (exchangeable Ca), mean annual precipitation (MAP), and maximum plant-available soil water content (AWC)] and vegetation attributes [community-weighted maximum diameter (CWM_{DMAX}), community-weighted mean wood density (CWM_{WD}), and functional richness (F_{RIC})] with above-ground biomass (AGB_W). Soil nutrient availability was significantly related to CWM_{DMAX}, CWM_{WD}, and AGB_W, and marginally to F_{RIC}. MAP and CWM_{DMAX} also significantly influenced AGB_W, while soil AWC and F_{RIC} showed marginal effects (dashed lines). Numbers (path coefficients, β) represent standardised regression weights. Black solid arrows indicate positive relationships, and the red arrow indicates a negative relationship. Except for AGB_W, all variables were standardised; therefore, model estimates are shown only for significant paths towards AGB_W to avoid misinterpretation.

Moreover, functional richness and maximum plant-available soil water showed marginally significant effects on AGB_W (β = 4.27, p = 0.082 for functional richness; and β = 5.69, p = 0.066 for maximum plant-available soil water). In the SEM framework, climatic water deficit did not affect vegetation traits or AGB_W (β = -0.33, p = 0.915). Finally, a significant negative covariance between community-weighted mean wood density and maximum stem diameter (estimate = -0.21; p = 0.037) was detected in the model, indicating that higher wood density is associated with smaller diameters. Significant variances in community-weighted mean wood density and maximum stem diameter, functional richness, and AGB_W point to considerable variability in the data.

Discussion

We aimed to identify the key environmental factors influencing above-ground woody biomass in the seasonally dry vegetation of the Caatinga region, addressing gaps in the literature by adopting standardised sampling and analysis protocols. Our research covers a large spatial scale, encompassing the largest and most continuous SDTF area in Latin America. We confirm our main hypothesis that, alongside climate, soils affect biomass directly and indirectly by mediating structural traits such as wood density and maximum stem diameter. This study highlights the critical role of soils in shaping vegetation properties in the dry tropics, providing new insights into the ecology of these understudied ecosystems.

Region-wide AGB_W is driven by complex soil–climate interactions

The AGB_W range in this study (4.87–85.65 Mg ha^{-1}) aligns with Santos et al. (2023), who reported similar values (2.85–80.88 Mg ha^{-1}) in seasonally dry vegetation of Bahia State, Brazil. Such variation reflects the spatial heterogeneity of the region, notably diverse edaphic conditions and distinct vegetation physiognomies. We highlighted that, while we cannot assert to what extent some of our study sites have undergone more drastic changes in the past, SDTFs are known for faster recovery after disturbances than moister forests due to their simpler structure (Josse and Balslev 1994; Pennington et al. 2006; Becknell et al. 2012).

Above-ground woody biomass in the Caatinga was shaped by both soil and climate, as well as their interactions (Fig. 2). Notably, MAP significantly influenced AGB_W only in a multivariate context, suggesting its effect is conditioned by other factors. This contrasts with the notion that, given the water-limited ecology of SDTFs, a coarse index like MAP is an adequate proxy for biomass content in these environments (Becknell et al. 2012). The MAP range in our study was on the drier end for global SDTFs, with 17 of 29 plots having MAP $\leq$ 800 mm yr^{-1}. Menezes et al. (2021) noted that Caatinga is even drier than Mexican 'very dry deciduous forests' studied by Lebrija-Trejos et al. (2008), where MAP lies around 900 mm yr^{-1}. While Becknell et al. (2012) noted a clear tendency of higher and lower above-ground biomass values above and below a MAP of 900 mm, respectively, our study did not confirm these differences, possibly due to the underrepresentation of high-MAP sites. The DryFlor Network (2016) sets an upper limit of 1800 mm MAP for SDTFs, but areas near this limit resemble semi-deciduous Atlantic forests. Cardoso et al. (2021) defined the 'core Caatinga' boundary

505 at 1300 mm MAP, above which distinct functional and floristic traits emerge. We reiterate that, while such
506 studies relate biomass to MAP, integrated metrics that incorporate potential evapotranspiration and soil water
507 availability may provide more informative insights in the Caatinga, where water availability is among the lowest
508 in the tropics.

509 We found no significant effect of temperature variables or elevation on AGB_W, in contrast to the
510 findings of Santos et al. (2023), who reported that MAP, MAT, and elevation together explained 46% of AGB_W
511 variation across sharp climatic and topographic gradients in Bahia's Chapada Diamantina. At the broader scale
512 of our study, other environmental drivers likely become more influential. In particular, soils with higher
513 maximum plant-available water may buffer the intense seasonal drought typical of the Caatinga. Although
514 shallow impermeable layers can retain moisture beyond the rainy season (Lloyd et al. 2015), rapid
515 evapotranspiration generally depletes these reserves in the Caatinga's shallow soils (Sampaio 2010). The
516 importance of water availability metrics observed in this study aligns with Terra et al. (2018), who demonstrated
517 that water availability is an important determinant of vegetation structure, function, and diversity across
518 Caatinga–Atlantic rainforest–Cerrado transitions.

519 Our results indicate that soil secondary macronutrients play an important role in shaping stand-level
520 AGB_W. Although required in smaller quantities than primary macronutrients (N, P, and K)|, secondary
521 macronutrients (Ca, Mg, and S) are essential to plant growth, metabolism, and structure (Marschner 2012).
522 Specifically, soil calcium was strongly supported in our modelling. Beyond its structural role in cell walls,
523 calcium enhances antioxidant activities during heat stress (Jiang and Huang 2001) and provides osmoprotection
524 under water deficit conditions (Jaleel et al. 2007). It also regulates a complex signalling network that helps
525 plants respond to various stresses (Tong et al. 2021), with its cytosolic concentration being linked to soil calcium
526 levels (Song et al. 2008; Sharma and Kumar 2021). Calcium is vital for root exocytosis and growth, enabling
527 roots to exploit soil resources (Wilkins et al. 2016), which may support the survival of Caatinga trees.
528 Furthermore, calcium plays a crucial role in multiple photosynthetic pathways by stomatal movement and
529 photosynthetic proteins (Wang et al., 2019). In contrast, our results indicate no significant role for magnesium
530 or potassium in determining AGB_W in Caatinga dry forests. Despite magnesium potentially alleviating
531 aluminium toxicity (Chen et al. 2018), this effect is unlikely to apply here due to the predominantly moderate
532 acid to alkaline soils found in our dataset. While potassium, in combination with plant-available soil water, has

been shown to positively influence tropical woody vegetation (CWAK hypothesis—Lloyd et al. 2015; Ametsitsi et al. 2020), these studies were conducted in forest-savanna ecotones with markedly different climate conditions and vegetation characteristics. Soil exchangeable sodium concentrations were minimal, with salinity not being an issue in most Caatinga soils (Pessoa et al. 2022).

Variations in total soil P and N concentrations appeared to have a limited impact on biomass stocks in our study plots, showing lower relative importance values in our analyses. Although total soil P does not represent readily available forms, it can reflect overall P availability and serve as a proxy in forest ecosystems (Quesada et al. 2010). Moreover, while only a small fraction of total soil P is directly available to plants, it may still indicate long-term P availability across stages of pedogenesis (Cross and Schlesinger 1995). Mechanisms such as 'P buffering capacity,' in which less bioavailable P pools are accessed during periods of scarcity (Kitayama et al. 2000; Quesada et al. 2010), remain unexplored in the Caatinga, despite its generally P-deficient soils (Sampaio 2010).

Regarding N, while many Caatinga legumes have the potential for biological nitrogen fixation (BNF), only a small fraction effectively fix nitrogen (Freitas et al. 2010; Silva et al. 2017), at least in part because BNF is an energy-intensive process (Gutschick 1981). Many legumes, particularly those in the Detarioideae and Caesalpinoideae subfamilies, cannot even nodulate (Sprent 2009), and no correlation between Fabaceae biomass and soil $\delta^{15}N$ (a potential indicator of the BNF degree) was observed by Brunello et al. (2024) for the same plots evaluated in this study. Studies on 'nutrient use efficiency' mechanisms (Vitousek 1982; 1984) could deepen our understanding of nutrient resorption from senescing leaves (Aerts 1996) in seasonal SDTFs. The soil N: P ratios found in this study suggest potential nutrient limitations. As an indicative metric, soil N: P ratios below 10 generally point to N limitation, whereas ratios above 20 suggest phosphorus limitation (Güsewell 2004). In our dataset, most sites were consistent with N limitation, although five values exceeded 20 (Table 1 of Online Resource 1), suggesting possible P limitation in some areas. Leaf nitrogen and phosphorus concentrations strongly influence photosynthetic traits, such as maximum carboxylation rate (V_{cmax}) (Walker et al., 2014), which in turn affects canopy growth. Therefore, variations in these nutrient levels may have influenced AGB_W depending on the plant species composition at each site, even though these patterns were not explored in detail in our analysis.

Finally, while differences in AGB_W were not statistically significant among geological substrates, a trend toward higher values in vegetation stands growing on carbonate-derived soils (S_{CAR}) was noticeable ('Karst' in Fig. 4-a of Online Resource 1). The lack of statistical significance might be due to the low number of observations in this category (n = 3). Recently, Muñoz et al. (2023) found that tropical dry forests growing on limestone-derived soils exhibit higher structural complexity and diversity (i.e., higher basal area, stand-level above-ground biomass, tree density, and species richness) compared to forests growing in phyllite-derived soils in southern Mexico.

Interestingly, AGB_W in GBR-01 was 58% higher than in GBR-02, despite both study plots sharing similar climatic and soil nutrient conditions. This difference may be related to the markedly shallower soil observed at GBR-02 (average depth = 28 cm), which could limit root anchorage and water storage. In contrast, the deeper soil at GBR-01 (average depth = 127 cm) likely offers greater physical support and functions as a larger reservoir for soil water. Within the S_{CAR} plots, PFF-01 exhibited the lowest AGB_W, even though it receives approximately 300 mm more annual precipitation than the other S_{CAR} sites. This discrepancy could be attributed to shallow or rocky soils, species composition effects, or potential unaccounted human disturbance, as the plot is located near small farms.

Relationships between soil properties and community functional composition

In this study, we found negative correlations between community-weighted wood density and several soil properties, notably exchangeable calcium, magnesium, potassium, zinc, and the silt fraction, while wood density was positively correlated with sand content (Fig. 7 of Online Resource 1). These correlations are likely to reflect hydraulic safety and water-use efficiency patterns. Specifically, low-wood-density species may have greater sapwood water capacitance, as wood density is generally correlated with xylem density. Low-density trees may store more water in their parenchymatic tissues, which are responsible for the storage of water, nutrients, and carbohydrates (Sarmiento et al. 2011; Lira-Martins et al. 2019). Osmotically active cations, such as potassium, improve water-use efficiency by enhancing plant cell capacitance (Quesada et al. 2012), which can be particularly important under water-limited conditions. An inverse relationship between wood density and these cations may indicate an evolutionary strategy in low-wood-density species, as a response to

anatomical constraints that increase embolism susceptibility, such as larger vessels (Lira-Martins et al. 2019). It is important to note that deciduousness is closely linked to embolism avoidance. However, evidence is not entirely consistent: Lima et al. (2018) demonstrated that lignin composition, rather than wood density alone, was the main factor explaining differences in xylem embolism resistance and leaf lifespan, with some high-wood-density species shedding their leaves earlier than expected. By contrast, other studies have suggested that high-wood-density species typically retain their leaves longer during dry periods and are generally considered the last to avoid embolism by shedding leaves, with their narrow vessels playing a crucial role in this process (Markesteijn et al. 2011; Lima et al., 2021). Noteworthily, leaf flushing is strongly dependent on soil water availability in the Caatinga (Paloschi et al. 2021). Lima et al. (2012) also identified distinct functional groups in the Caatinga, i.e., evergreen, low-wood-density, and high-wood-density species, and showed that phenological events (leaf flush and flowering) are driven by water availability in high-wood-density species and by photoperiod in low-wood-density species.

Regarding the inverse relationship between soil zinc and wood density, zinc has been shown to enhance the activity of osmoregulation substances during drought stress (Wu et al. 2015). This suggests that zinc likely participates in structural and biochemical trade-offs within cells, potentially improving drought resilience. Soil texture also influenced wood density, with sand content showing a positive association and silt content a negative association. This relationship may be difficult to interpret due to the strong correlation between soil texture and cation availability (Table 4 of Online Resource 1), which complicates the separation of their individual effects. However, soil texture is known to influence plant and soil hydraulic properties, as well as tree mechanical stability, factors that can affect wood density (Quesada et al. 2012). Moreover, the observed positive association between sand content and community wood density (Fig. 7 of Online Resource 1) may reflect an adaptive strategy whereby trees tolerate and cope with, rather than avoid, water scarcity. In coarse-textured soils, water drains more rapidly, and nutrient retention may be lower. Thus, species with denser wood may be favoured due to their ability to withstand drought stress under such conditions.

Maximum stem diameters were positively associated with stand functional richness, suggesting that stands with larger trunks also occupy more niche space. Soil properties, specifically exchangeable calcium and the sum of bases, are significantly related to maximum stem diameter, highlighting the importance of soil bases for secondary growth, as already observed in other Brazilian dry forests (Angélico et al. 2021).

615 The relationships between functional richness and all measured soil cations (excluding exchangeable
616 aluminium) suggest that variations in soil properties may drive differences in plant physiology and anatomy,
617 yielding optimal trade-offs between secondary growth and water-use efficiency strategies. Our results suggest
618 that increased soil nutrient availability across different geological formations in the Caatinga enables a broader
619 range of conservative and acquisitive strategies, as reflected in the community functional properties studied
620 here, thereby maximising functional diversity at the regional scale.
621
622 Soil-mediated effects of functional assemblage on above-ground woody biomass

623 Our Structural Equation Model (SEM; Fig. 5) highlights how soil properties, specifically nutrient
624 availability, indirectly shape biomass by mediating community functional composition. The SEM shows that
625 soil nutrient availability, tree diameter, and mean annual precipitation are crucial for stand-level biomass
626 accumulation in the Caatinga region. Specifically, soil calcium not only directly impacts above-ground biomass
627 through mechanisms already discussed in the previous sections, but also influences wood density, maximum
628 stem diameter, and functional richness, aligning with previous studies on the role of soil nutrients in vegetation
629 structure and community assembly in the Caatinga region (Souza et al. 2019; Oliveira et al. 2019; Maia et al.
630 2020).

631 Considering its effect size, the community-weighed maximum stem diameter was the strongest
632 predictor of biomass, consistent with the 'biomass ratio' hypothesis (Grime 1998), in which predominant traits
633 are crucial for determining vegetation stand-level attributes in a given community. This suggests that the
634 abundance of typically larger species reflects biomass patterns at the stand level. Rather than serving solely as
635 a biomass predictor, community-weighted maximum stem diameter captures ecological filtering, reflecting the
636 ability of certain species to establish and dominate in the community. In the SEM, mean annual precipitation
637 influenced biomass positively alongside other variables, underscoring the importance of rainfall totals for
638 biomass accumulation, as comprehensively discussed in this paper. However, variables related to water
639 availability, such as climatic water deficit and maximum plant-available soil water, showed weaker or no
640 significant effects on biomass in the SEM. The multi-model inference framework tested a broader set of
641 environmental variables, including interaction terms, while the SEM provides a more integrative picture of the

642 relationships among environmental and vegetation variables. These approaches were conceived as
643 complementary rather than directly comparable.

644 The inverse relationship found between wood density and maximum stem diameter indicates that
645 thicker trees tend to have lower wood densities, which may reflect different plant life-history strategies. Wood
646 density is linked to plant hydraulic safety and construction costs, with thicker trunks often resulting in higher
647 respiration costs, which may not be optimal for Caatinga trees (Bosc et al. 2003; Larjavaara and Muller-Landau
648 2010). Additionally, wood density has been strongly associated with mortality rates in tropical forests, with
649 higher survival rates generally associated with denser wood (Kraft et al., 2010). Alongside these findings, it is
650 worth noting that although our study plots are considered structurally mature, older, thicker trees are relatively
651 rare in many areas of the Caatinga due to chronic wood extraction by local communities.

652 The functional richness index exhibited only a weak, marginally positive association with AGB_W,
653 providing little support for the niche complementarity hypothesis (Tilman 1999). Despite this marginal effect,
654 our result contrasts with the findings of Prado-Junior et al. (2016), who observed a positive effect of functional
655 divergence and evenness on biomass, rather than functional richness. Their study suggested that communities
656 with functionally distinct, yet evenly abundant individuals, are more likely to exhibit higher biomass over time.
657 Prado-Junior et al. (2016) included specific leaf area (SLA) in their functional diversity index, although this
658 trait was less significant in explaining biomass in their work.

659

660 Caveats and future directions

661 Our *Space-for-Time* approach (Pickett 1989) supports existing ecological hypotheses while contrasting
662 others. For example, we found no significant impact of the maximum temperature of the warmest month on
663 AGB_W in the Caatinga. High temperatures can induce tree mortality via hydraulic failure and carbon starvation
664 (McDowell et al. 2018), but the Caatinga flora is adapted to endure extreme heat and drought. High temperatures
665 also affect photosynthesis via stomatal closing, which depends on the optimal/maximum values for each
666 species. Adaptive mechanisms include deciduousness, leaf trait modifications, osmoprotectant accumulation
667 (Medina 1983; Mathur et al. 2014; Jajoo and Allakhverdiev 2017), deeper root systems, and arbuscular

668 mycorrhizal associations (Hodge 2009; Smith and Smith 2011). However, the lack of temporal data limits our
669 conclusions. Long-term monitoring is crucial for accurately assessing the impact of temperature and other
670 environmental variables on vegetation structure and functioning in SDTFs.

671 While AGB_W values were not significantly influenced by the RSGs, clay mineral types, or geological
672 substrates evaluated here, we do not generalise these findings to the entire region. A broader sampling
673 incorporating more observations, a wider range of clay mineral proportions, additional RSGs (e.g., Ferralsols),
674 and geological substrates would be necessary to more comprehensively test this hypothesis.

675 Another limitation of the current approach is that the estimation of maximum plant-available soil
676 water does not account for stoniness. The presence of stones and rock fragments was recorded only semi-
677 quantitatively during field sampling, making it unsuitable for volume correction without introducing
678 considerable uncertainty. Additionally, the pedotransfer function employed was not calibrated to accommodate
679 significant coarse fragment content. While the work of Saxton and Rawls (2006) incorporates rock fragment
680 corrections, it is not considered appropriate for the edaphoclimatic conditions of the semi-arid Caatinga. It is
681 also important to note that most of our study sites are located in sedimentary terrains, where stoniness is
682 generally negligible or absent. In crystalline landscapes, although rock fragments may be more frequent, the
683 depth of soil is likely the primary constraint on plant-available water storage. Future work could benefit from
684 more detailed assessments of coarse fragment contents and their implications for water retention, particularly
685 in rocky landscapes.

686 Although our SEM demonstrated reasonably good fit indices, it is important to acknowledge the
687 exploratory nature of the model and its relatively small sample size, which can reduce statistical power and
688 increase the risk of Type II errors, where true relationships may go undetected. A larger sample size would
689 strengthen the robustness of the estimates and enhance the generalisability of the findings. Furthermore, while
690 the model tested various explanatory pathways, incorporating additional environmental variables or alternative
691 pathways could reveal relationships not captured in the current analysis. Therefore, future studies with larger
692 datasets are needed to disentangle other intricate relationships among environmental factors, ecosystem
693 structure, and functioning. Furthermore, future studies should explore the role of clay mineralogy on soil
694 hydraulic properties (water retention curve and hydraulic conductivity) and related effects on root zone storage

and root water uptake, as well as on root viability, which could enhance plant resilience under water-limited conditions. Finally, given the significant environmental heterogeneity of the Caatinga region and its long history of human alterations, caution is needed to avoid overgeneralising our results.

Conclusions

Our study unravels the complex interplay between climate, soil properties, and vegetation properties in SDTFs of the Caatinga region. The multi-model inference approach employed proved effective in capturing these relationships, while the structural equation model provided a comprehensive picture of how environmental factors and functional attributes collectively influence above-ground woody biomass.

Soil nutrient availability, mean annual precipitation, and the interaction between climatic and edaphic factors emerged as key drivers of above-ground woody biomass in the Caatinga. Beyond their direct influence on stand-level biomass, soil cations played a significant role in shaping community-weighted traits and functional richness. In synthesis, more favourable soil conditions (i.e., higher nutrient availability and greater water storage capacity) and higher mean annual precipitation, altogether, positively influenced above-ground woody biomass.

While our study provides valuable insights into the ecology of SDTFs, limitations such as a relatively small sample size and the absence of temporal data restrict the generalisability of our findings. Nevertheless, our research advances understanding of the role of functional attributes in AGB_W accumulation patterns within SDTFs, supporting the forecasting of potential tipping points and ecosystem state shifts, as highlighted by Muñoz et al. (2023). These findings carry important implications for biodiversity conservation and carbon sequestration initiatives in dry tropical regions, offering guidance for policymaking in the face of global environmental change.

Acknowledgements

We thank Associação Caatinga for permitting data collection at RPPN Serra das Almas, Fundação Biodiversitas for supporting fieldwork in Boa Vista do Tupim and Canudos (Bahia), and the State Forestry Institute (IEF) of Minas Gerais for assistance at Lagoa do Cajueiro State Park. We are grateful to the following individuals: Jonas O. Moraes Filho, Erison Gomes, Raimundo Nonato de Araújo Filho, Laura Oliveira, José Edivaldo Chaves, Euvaldo Júnior, Rodrigo Miranda, Antônio Belo, Luiz Dez (Gruta dos Brejões), Eudes Velozo (Fazenda Esperança), Glaucia Drummond, Pierre Landolt (Fazenda Tamanduá), Bruno Menezes, and Joabe Santos de Almeida. Finally, we thank Professor Everardo V. S. B. Sampaio for kindly reviewing a previous version of this manuscript.

References

Aerts R (1996) Nutrient resorption from senescing leaves of perennials: Are there general patterns? J Ecol 84:597. https://doi.org/10.2307/2261481

Ametsitsi GKD, Van Langevelde F, Logah V, et al (2020) Fixed or mixed? Variation in tree functional types and vegetation structure in a forest-savanna ecotone in West Africa. J Trop Ecol. https://doi.org/10.1017/S0266467420000085

Andrade GO de (1977) Alguns aspectos do quadro natural do Nordeste. Série B: Brasil. SUDENE, Estudos Regionais 2, pp 1–39.

Angélico TS, Marcati CR, Rossi S, da Silva MR, Sonsin-Oliveira J (2021) Soil effects on stem growth and wood anatomy of tamboril are mediated by tree age. Forests 12:1058. https://doi.org/10.3390/f12081058

Araujo HFP, Canassa NF, Machado CCC, Tabarelli M (2023) Human disturbance is the major driver of vegetation changes in the Caatinga dry forest region. Sci Rep 13:1–11. https://doi.org/10.1038/s41598-023-45571-9

Bartón K (2020) MuMIn: Multi-Model Inference. R package version 1.43.17. https://cran.r-project.org/package=MuMIn

Bauman D, Drouet T, Dray S, Vleminckx J (2018a) Disentangling good from bad practices in the selection of spatial or phylogenetic eigenvectors. Ecography 41:1638–1649. https://doi.org/10.1111/ecog.03380

Bauman D, Drouet T, Fortin MJ, Dray S (2018b) Optimizing the choice of a spatial weighting matrix in eigenvector-based methods. Ecology 99:2159–2166. https://doi.org/10.1002/ecy.2469

Becknell JM, Kucek LK, Powers JS (2012) Aboveground biomass in mature and secondary seasonally dry tropical forests: A literature review and global synthesis. For Ecol Manag 276:88–95. https://doi.org/10.1016/j.foreco.2012.03.033

Bosc A, De Grandcourt A, Loustau D (2003) Variability of stem and branch maintenance respiration in a Pinus pinaster tree. Tree Physiol 23:227–236. https://doi.org/10.1093/treephys/23.4.227

Brown S, Lugo AE (1982) The storage and production of organic matter in tropical forests and their role in the global carbon cycle. Biotropica 14:161. https://doi.org/10.2307/2388024

Browne MW, Cudeck R (1992) Alternative ways of assessing model fit. Sociol Methods Res 21:136–160.

Brunello AT, Nardoto GB, Santos FLS, Sena-Souza JP, Quesada CAN, Lloyd JJ, Domingues TF (2024) Soil $\delta^{15}N$ spatial distribution is primarily shaped by climatic patterns in the semiarid Caatinga, Northeast Brazil. Sci Total Environ 908:168405. https://doi.org/10.1016/j.scitotenv.2023.168405

Burnham KP, Anderson DR, Huyvaert KP (2011) AIC model selection and multimodel inference in behavioral ecology: Some background, observations, and comparisons. Behav Ecol Sociobiol 65(1):23–35. https://doi.org/10.1007/s00265-010-1029-6

Cardoso D, Moonlight PW, Ramos G, et al (2021) Defining Biologically Meaningful Biomes Through Floristic, Functional, and Phylogenetic Data. Front Ecol Evol 9:1–16. https://doi.org/10.3389/fevo.2021.723558

Carvalho G (2020) flora: Tools for interacting with the Brazilian Flora 2020. R package version 0.3.4. https://CRAN.R-project.org/package=flora

Castanho ADA, Coe MT, Brando P, Macedo M, Baccini A, Walker W, Andrade EM (2020) Potential shifts in the aboveground biomass and physiognomy of a seasonally dry tropical forest in a changing climate. Environ Res Lett 15:034053. https://doi.org/10.1088/1748-9326/ab7394

Chave J, Coomes D, Jansen S, Lewis SL, Swenson NG, Zanne AE (2009) Towards a worldwide wood economics spectrum. Ecol Lett 12(4):351–366. https://doi.org/10.1111/j.1461-0248.2009.01285.x

Chave J, Réjou-Méchain M, Búrquez A, Chidumayo E, Colgan MS, Delitti WBC, Duque A, Eid T, Fearnside PM, Goodman RC, Henry M, Martínez-Yrízar A, Mugasha WA, Muller-Landau HC, Mencuccini M, Nelson BW, Ngomanda A, Nogueira EM, Ortiz-Malavassi E, … Vieilledent G (2014) Improved allometric models to estimate the aboveground biomass of tropical trees. Glob Change Biol 20(10):3177–3190. https://doi.org/10.1111/gcb.12629

Chen ZC, Peng WT, Li J, Liao H (2018) Functional dissection and transport mechanism of magnesium in plants. Semin Cell Dev Biol 74:142–152. https://doi.org/10.1016/j.semcdb.2017.08.005

Corona-Núñez RO, Campo J, Williams M (2018) Aboveground carbon storage in tropical dry forest plots in Oaxaca, Mexico. For Ecol Manage 409(18):202–214. https://doi.org/10.1016/j.foreco.2017.11.014

Cross AF, Schlesinger WH (1995) A literature review and evaluation of the Hedley fractionation: applications to the biogeochemical cycle of soil phosphorus in natural ecosystems. Geoderma 64:197–214. https://doi.org/10.1016/0016-7061(94)00023-4

Dray AS, Bauman D, Blanchet G, Borcard D, Clappe S, Guenard G, Jombart T, Larocque G, Legendre P, Madi N, Wagner HH (2021) Package 'adespatial.' https://doi.org/10.1890/11-1183.1

DRYFLOR (Banda-R K, Delgado-Salinas A, Dexter KG, Linares-Palomino R, Oliveira-Filho A, Prado D, Pullan M, Quintana C, Riina R, Rodríguez MG, Weintritt J, Acevedo-Rodríguez P, Adarve J, Álvarez E, Aranguren B A, Arteaga JC, Aymard G, Castaño A, Ceballos-Mago N, … Pennington RT) (2016) Plant diversity patterns in neotropical dry forests and their conservation implications. Science 353(6306):1383–1387. https://doi.org/10.1126/science.aaf5080

Fernandes MF, Cardoso D, de Queiroz LP (2020) An updated plant checklist of the Brazilian Caatinga seasonally dry forests and woodlands reveals high species richness and endemism. J Arid Environ 174:104079. https://doi.org/10.1016/j.jaridenv.2019.104079

Fick SE, Hijmans RJ (2017) WorldClim 2: New 1-km spatial resolution climate surfaces for global land areas. Int J Climatol 37(12):4302–4315. https://doi.org/10.1002/joc.5086

Freitas ADS, Sampaio EVSB, Santos CER, Fernandes AR (2010) Biological nitrogen fixation in tree legumes of the Brazilian semi-arid caatinga. J Arid Environ 74(3):344–349. https://doi.org/10.1016/j.jaridenv.2009.09.018

Furley PA, Ratter JA (1988) Soil resources and plant communities of the Central Brazilian Cerrado and their development. J Biogeogr 15(1):97. https://doi.org/10.2307/2845050

Gee GW, Bauder JW (1986) Particle-size analysis. In: Klute A (ed) Methods of Soil Analysis, Part 1: Physical and Mineralogical Methods. 2nd ed. American Society of Agronomy, Madison, WI, pp 383–411

Glenday J (2008) Carbon storage and emissions offset potential in an African dry forest, the Arabuko-Sokoke Forest, Kenya. Environ Monit Assess 142(1–3):85–95. https://doi.org/10.1007/s10661-007-9910-0

Grime JP (1998) Benefits of plant diversity to ecosystems: Immediate, filter, and founder effects. J Ecol 86(6):902–910. https://doi.org/10.1046/j.1365-2745.1998.00306.x

Güsewell S (2004) N:P ratios in terrestrial plants: Variation and functional significance. New Phytologist 164:243–266

Gutschick VP (1981) Evolved strategies in nitrogen acquisition by plants. Am Nat 118(5):607–637. https://doi.org/10.1086/283858

Harrison XA, Donaldson L, Correa-Cano ME, Evans J, Fisher DN, Goodwin CED, Robinson BS, Hodgson DJ, Inger R (2018) A brief introduction to mixed effects modelling and multi-model inference in ecology. PeerJ 6:e4794. https://doi.org/10.7717/peerj.4794

Hodnett MG, Tomasella J (2002) Marked differences between van Genuchten soil water-retention parameters. Geoderma 108:155–180

Hodge A (2009) Root decisions. Plant Cell Environ 32(6):628–640. https://doi.org/10.1111/j.1365-3040.2008.01891.x

IBGE (2019) Biomas e Sistema Costeiro-Marinho do Brasil: compatível com a escala 1:250.000. Brazilian Institute of Geography and Statistics, Rio de Janeiro

Jajoo A, Allakhverdiev SI (2017) High-temperature stress in plants: Consequences and strategies for protecting photosynthetic machinery. In: Shabala S (ed) Plant Stress Physiology, 2nd ed. CABI, pp 138–154. https://doi.org/10.1079/9781780647296.0279

Jaleel CA, Manivannan P, Sankar B, Kishorekumar A, Gopi R, Somasundaram R, Panneerselvam R (2007) Water deficit stress mitigation by calcium chloride in Catharanthus roseus: Effects on oxidative stress, proline metabolism, and indole alkaloid accumulation. Colloids Surf B Biointerfaces 60(1):110–116. https://doi.org/10.1016/j.colsurfb.2007.06.006

Jiang Y, Huang B (2001) Effects of calcium on antioxidant activities and water relations associated with heat tolerance in two cool-season grasses. J Exp Bot 52(355):341–349. https://doi.org/10.1093/jxb/52.355.341

Josse C, Balslev H (1994) The composition and structure of a dry, semideciduous forest in western Ecuador. Nordic J Bot 14(4):425–434. https://doi.org/10.1111/j.1756-1051.1994.tb00628.x

King DA, Davies SJ, Noor NSM (2006) Growth and mortality are related to adult tree size in a Malaysian mixed dipterocarp forest. Forest Ecol Manag 223(1–3):152–158. https://doi.org/10.1016/j.foreco.2005.10.066

Kitayama K, Majalap-Lee N, Aiba S (2000) Soil phosphorus fractionation and phosphorus-use efficiencies of tropical rainforests along altitudinal gradients of Mount Kinabalu, Borneo. Oecologia 123(3):342–349. https://doi.org/10.1007/s004420051020

Kraft NJB, Metz MR, Condit RS, Chave J (2010) The relationship between wood density and mortality in a global tropical forest data set. New Phytologist 188:1124–1136. https://doi.org/10.1111/j.1469-8137.2010.03444.x

Laliberté AE, Legendre P, Shipley B (2014) FD: Measuring Functional Diversity from Multiple Traits, and Other Tools for Functional Ecology. R package version 1.0-12.1. Available at https://cran.r-project.org/web/packages/FD/index.html

Larjavaara M, Muller-Landau HC (2010) Rethinking the value of high wood density. Funct Ecol 24(4):701–705. https://doi.org/10.1111/j.1365-2435.2010.01698.x

Lebrija-Trejos E, Bongers F, Pérez-García EA, Meave JA (2008) Successional change and resilience of a very dry tropical deciduous forest following shifting agriculture. Biotropica 40(4):422–431. https://doi.org/10.1111/j.1744-7429.2008.00398.x

Lehmann, P, Leshchinsky, B, Gupta, S, Mirus, BB, Bickel, S, Lu, N, Or, D. (2021) Clays are not created equal: How clay mineral type affects soil parameterization. Geophysical Research Letters, 48(20), e2021GL095311. https://doi.org/10.1029/2021GL095311

Lima ALA de, de Sá Barretto Sampaio EV, de Castro CC, et al (2012) Do the phenology and functional stem attributes of woody species allow for the identification of functional groups in the semiarid region of Brazil? Trees - Structure and Function 26:1605–1616. https://doi.org/10.1007/s00468-012-0735-2

Lima TRA, Carvalho ECD, Martins FR, et al (2018) Lignin composition is related to xylem embolism resistance and leaf life span in trees in a tropical semiarid climate. New Phytologist 219:1252–1262. https://doi.org/10.1111/nph.15211

Lima ALA de, Rodal MJN, Castro CC, et al (2021) Phenology of high- and low-density wood deciduous species responds differently to water supply in tropical semiarid regions. J Arid Environ 193:. https://doi.org/10.1016/j.jaridenv.2021.104594

Lira-Martins D, Humphreys-Williams E, Strekopytov S, Ishida FY, Quesada CA, Lloyd J (2019) Tropical tree branch-leaf nutrient scaling relationships vary with sampling location. Front Plant Sci 10:877. https://doi.org/10.3389/fpls.2019.00877

Lloyd J, Domingues TF, Schrodt F, Ishida FY, Feldpausch TR, Saiz G, Quesada CA, Schwarz M, Torello-Raventos M, Gilpin M, Marimon BS, Marimon-Junior BH, Ratter JA, Grace J, Nardoto GB, Veenendaal E, Arroyo L, Villarroel D, Killeen TJ, et al. (2015) Edaphic, structural and physiological contrasts across Amazon Basin forest-savanna ecotones suggest a role for potassium as a key modulator of tropical woody vegetation structure and function. Biogeosciences 12(22):6529–6571. https://doi.org/10.5194/bg-12-6529-2015

Lloyd J, Goulden ML, Ometto JP, Patiño S, Fyllas NM, Quesada CA (2009) Ecophysiology of forest and savanna vegetation. In: Keller M, Bustamante M, Gash J, Dias PS (eds) Amazonia and Global Change, pp 463–484. American Geophysical Union. https://doi.org/10.1029/2008GM000740

Londe V, Gomes PWP, Martins FR (2023) The role of edaphic differentiation on life zones, vegetation types, β-diversity, and indicator species in tropical dry forests. Plant Soil 493(1–2):573–588. https://doi.org/10.1007/s11104-023-06249-3

Maia VA, de Souza CR, de Aguiar-Campos N, Fagundes NCA, Santos ABM, de Paula GGP, Santos PF, Silva WB, de Oliveira Menino GC, dos Santos RM (2020) Interactions between climate and soil shape tree community assembly and above-ground woody biomass of tropical dry forests. Forest Ecol Manag 474:118348. https://doi.org/10.1016/j.foreco.2020.118348

Marschner P (2012) Marschner's Mineral Nutrition of Higher Plants, 3rd edn. Academic Press, London

Markesteijn L, Poorter L, Paz H, Sack L, Bongers F (2011) Ecological differentiation in xylem cavitation resistance is associated with stem and leaf structural traits. Plant Cell Environ 34(1):137–148. https://doi.org/10.1111/j.1365-3040.2010.02231.x

Mason NWH, Mouillot D, Lee WG, Wilson JB (2005) Functional richness, functional evenness and functional divergence: The primary components of functional diversity. Oikos 111(1):112–118. https://doi.org/10.1111/j.0030-1299.2005.13886.x

Mathur S, Agrawal D, Jajoo A (2014) Photosynthesis: Response to high-temperature stress. J Photochem Photobiol B: Biol 137:116–126. https://doi.org/10.1016/j.jphotobiol.2014.01.010

Max A, Wing J, Weston S, et al. (2020) caret: Classification and regression training. R package version 6.0-94. https://cran.r-project.org/web/packages/caret/caret.pdf

Mazerolle MJ (2023) Model selection and multimodel inference using the AICcmodavg package. In: AICcmodavg: Model selection and multimodel inference based on (Q)AIC(c). R package version 2.3-1. https://cran.r-project.org/web/packages/AICcmodavg/vignettes/AICcmodavg.pdf

McDowell N, Allen CD, Anderson-Teixeira K, et al. (2018) Drivers and mechanisms of tree mortality in moist tropical forests. New Phytol 219(3):851–869. https://doi.org/10.1111/nph.15027

Medina E (1983) Adaptations of tropical trees to moisture stress. In: Ecosystems of the World: Tropical Rain Forest Ecosystems, pp 225–237.

Menezes RSC, Sales AT, Primo DC, et al. (2021) Soil and vegetation carbon stocks after land-use changes in a seasonally dry tropical forest. Geoderma 390:114943. https://doi.org/10.1016/j.geoderma.2021.114943

Miles L, Newton AC, DeFries RS, et al. (2006) A global overview of the conservation status of tropical dry forests. J Biogeogr 33(3):491–505. https://doi.org/10.1111/j.1365-2699.2005.01424.x

Moonlight P, Banda-R K, Phillips OL, et al. (2021) Supplementary Material: The DryFlor field manual for plot establishment and remeasurement. Plants People Planet 3:295–300. http://www.dryflor.info/files/ppp310112-sup-0001-supinfo_english.pdf

Moonlight PW, Banda-R K, Phillips OL, et al. (2021) Expanding tropical forest monitoring into Dry Forests: The DRYFLOR protocol for permanent plots. Plants People Planet 3(3):295–300. https://doi.org/10.1002/ppp3.10112

Muñoz R, Enríquez M, Bongers F, et al (2023) Lithological substrates influence tropical dry forest structure, diversity, and composition, but not its dynamics. Frontiers in Forests and Global Change 6:. https://doi.org/10.3389/ffgc.2023.1082207

Murphy PG, Lugo AE (1986) Ecology of tropical dry forest. Annu Rev Ecol Syst 17(1):67–88. https://doi.org/10.1146/annurev.es.17.110186.000435

Ocón JP, Ibanez T, Franklin J, et al. (2021) Global tropical dry forest extent and cover: A comparative study of bioclimatic definitions using two climatic data sets. PLoS ONE 16(5):e0252063. https://doi.org/10.1371/journal.pone.0252063

O'Donnell MS, Ignizio DA (2012) Bioclimatic Predictors for Supporting Ecological Applications in the Conterminous United States. U.S Geological Survey Data Series 691. https://doi.org/10.3133/ds691

Oliveira OF de (2011) Caatinga of Northeastern Brazil: Vegetation and floristic aspects. In: Riet-Correa F, Pfister J, Schild AL, Wierenga T (eds) Poisoning by Plants, Mycotoxins, and Related Toxins. CAB International, pp 2–24.

Oliveira G de, Araújo MB, Rangel TF, et al. (2012) Conserving the Brazilian semiarid (Caatinga) biome under climate change. Biodivers Conserv 21(11):2913–2926. https://doi.org/10.1007/s10531-012-0346-7

Oliveira GC, Francelino MR, Arruda DM, et al. (2019) Climate and soils at the Brazilian semiarid and the forest-Caatinga problem: New insights and implications for conservation. Environ Res Lett 14(10):104007. https://doi.org/10.1088/1748-9326/ab3d7b

Olsen SR, Sommers LE (1982) Phosphorus. In: Page AL (ed) Methods of Soil Analysis, 2nd ed. American Society of Agronomy/Soil Science Society of America, Madison, pp 403–427.

Paloschi RA, Ramos DM, Ventura DJ, Souza R, Souza E, Morellato LPC, Nóbrega RLB, Coutinho IAC, Verhoef A, Körting TS, Borma LDS (2021) Environmental drivers of water use for caatinga woody plant species: Combining remote sensing phenology and sap flow measurements. Remote Sens 13(1):75. https://doi.org/10.3390/rs13010075

Pastor J, Aber JD, McClaugherty CA, Melillo JM (1984) Above-ground production and N and P cycling along a nitrogen mineralization gradient on Blackhawk Island, Wisconsin. Ecology 65:256–268.

Pateiro-Lopez B, Rodriguez-Casal A (2019) alphahull: Generalization of the convex hull of a sample of points in the plane. R package version 2.2. https://CRAN.R-project.org/package=alphahull

Pennington RT, Ratter JA, Lewis GP (2006) An overview of the plant diversity, biogeography and conservation of neotropical savannas and seasonally dry forests. In: Pennington RT, Lewis GP, Ratter JA (eds) Neotropical savannas and seasonally dry forests: plant diversity, biogeography and conservation. CRC Press, Florida, pp 1–29.

Pessoa LGM, Freire MBG dos S, Green CHM, et al (2022) Assessment of soil salinity status under different land-use conditions in the semiarid region of Northeastern Brazil. Ecol Indic 141:. https://doi.org/10.1016/j.ecolind.2022.109139

Pickett STA (1989) Space-for-time substitution as an alternative to long-term studies. In: Long-Term Studies in Ecology, pp 110–135. https://doi.org/10.1007/978-1-4615-7358-6_5

Pleysier JL, Juo ASR (1980) A single-extraction method using silver-thiourea for measuring exchangeable cations and effective CEC in soils with variable charges. Soil Sci 129:205–211.

Prado-Junior JA, Schiavini I, Vale VS, Arantes CS, van der Sande MT, Lohbeck M, Poorter L (2016) Conservative species drive biomass productivity in tropical dry forests. J Ecol 104(3):817–827. https://doi.org/10.1111/1365-2745.12543

Queiroz LP de, Cardoso D, Fernandes MF, Moro MF (2017) Diversity and evolution of flowering plants of the Caatinga domain. In: Silva JMC da, Leal IR, Tabarelli M (eds) Caatinga: The Largest Tropical Dry Forest Region in South America. Springer. https://doi.org/10.1007/978-3-319-68339-3

Quesada CA, Lloyd J, Schwarz M, Patiño S, Baker TR, Czimczik C, Fyllas NM, Martinelli L, Nardoto GB, Schmerler J, Santos AJB, Hodnett MG, Herrera R, Luizão FJ, Arneth A, Lloyd G, Dezzeo N, Hilke I, Kuhlmann I, … Paiva R (2010) Variations in chemical and physical properties of Amazon forest soils in relation to their genesis. Biogeosciences 7(5):1515–1541. https://doi.org/10.5194/bg-7-1515-2010

Quesada CA, Phillips OL, Schwarz M, et al (2012) Basin-wide variations in Amazon forest structure and function are mediated by both soils and climate. Biogeosciences 9:2203–2246. https://doi.org/10.5194/bg-9-2203-2012

Quesada CA, Paz C, Oblitas Mendoza E, Phillips OL, Saiz G, Lloyd J (2020) Variations in soil chemical and physical properties explain basin-wide Amazon forest soil carbon concentrations. SOIL 6(1):53–88. https://doi.org/10.5194/soil-6-53-2020

R Core Team (2021) R: A Language and Environment for Statistical Computing. R Foundation for Statistical Computing. Retrieved from https://www.r-project.org/

Ratter JA, Richards PW, Argent G, Gifford DR (1973) Observations on the vegetation of northeastern Mato Grosso: I. The woody vegetation types of the Xavantina-Cachimbo Expedition Area. Philos Trans R Soc Lond B Biol Sci 266(880):449–492. https://doi.org/10.1098/rstb.1973.0053

Ratter JA, Askew GP, Montgomery RF, Gifford DR (1978) Observations on forests of some mesotrophic soils in Central Brazil. Rev Bras Bot 1:47–58.

Reich PB (2014) The world-wide "fast-slow" plant economics spectrum: A traits manifesto. J Ecol 102(2):275–301. https://doi.org/10.1111/1365-2745.12211

Righi D, Meunier A (1995) Origin and Mineralogy of Clays. In: Velde B (ed) Origin and Mineralogy of Clays. Springer, Berlin Heidelberg. https://doi.org/10.1007/978-3-662-12648-6

Roa-Fuentes LL, Campo J, Parra-Tabla V (2012) Plant biomass allocation across a precipitation gradient: An approach to seasonally dry tropical forest at Yucatán, Mexico. Ecosystems 15(8):1234–1244. https://doi.org/10.1007/s10021-012-9578-3

Rosseel Y (2012) lavaan: An R package for structural equation modeling. J Stat Softw 48:1–36. https://doi.org/10.18637/jss.v048.i02

Saldarriaga JG, West DC, Tharp ML, Uhl C (1988) Long-term chronosequence of forest succession in the Upper Rio Negro of Colombia and Venezuela. J Ecol 76(4):938. https://doi.org/10.2307/2260625

Sampaio EVSB (1995) Overview of the Brazilian Caatinga. In: Mooney HA, Bullock SH, Medina E (eds) Seasonally Dry Tropical Forests. Cambridge University Press, pp 35–63. https://doi.org/10.1017/CBO9780511753398.003

Sampaio EVSB, Silva GC (2005) Equações para estimar a biomassa de plantas da caatinga do semi-árido brasileiro. Acta Bot Bras 19(4):935–943. https://doi.org/10.1590/S0102-33062005000400028

Sampaio Everardo Valadares Sá Barretto (2010) Caracterização do bioma caatinga: características e potencialidades. In: Gariglio MA, de S. B. S. L. A. Cestaro, Kageyama PY (eds) Uso sustentável e conservação dos recursos florestais da caatinga. MMA, pp 29–48.

Santos HKV, Borges de Lima R, Figueiredo de Souza RL, Cardoso D, Moonlight PW, Teixeira Silva T, Pereira de Oliveira C, Alves Júnior FT, Veenendaal E, de Queiroz LP, Rodrigues PMS, Dos Santos RM, Sarkinen T, de Paula A, Barreto-Garcia PAB, Pennington T, Phillips OL (2023) Spatial distribution of aboveground biomass stock in tropical dry forest in Brazil. IForest 16(2):116–126. https://doi.org/10.3832/ifor4104-016

Sarmiento C, Patiño S, Timothy Paine CE, Beauchêne J, Thibaut A, Baraloto C (2011) Within-individual variation of trunk and branch xylem density in tropical trees. Am J Bot 98(1):140–149. https://doi.org/10.3732/ajb.1000034

Saxton KE, Rawls WJ (2006) Soil Water Characteristic Estimates by Texture and Organic Matter for Hydrologic Solutions. Soil Science Society of America Journal 70:1569–1578. https://doi.org/10.2136/sssaj2005.0117

Sharma D, Kumar A (2021) Calcium signaling network in abiotic stress tolerance in plants. In: AUTHORS/Editors of Book Calcium Transport Elements in Plants, Vol. 2. Elsevier Inc. https://doi.org/10.1016/b978-0-12-821792-4.00003-5

Silva AF da, Freitas AD S de, Costa TL, Fernandes-Júnior PI, Martins LM V, Santos CE de R e S, Menezes KA S, Sampaio EV de S B (2017) Biological nitrogen fixation in tropical dry forests with different legume diversity and abundance. Nutr Cycl Agroecosyst 107(3):321–334. https://doi.org/10.1007/s10705-017-9834-1

Smith SE, Smith FA (2011) Roles of arbuscular mycorrhizas in plant nutrition and growth: New paradigms from cellular to ecosystem scales. Annu Rev Plant Biol 62:227–250. https://doi.org/10.1146/annurev-arplant-042110-103846

Song WY, Zhang Z Bin, Shao HB, Guo XL, Cao HX, Zhao H Bin, Fu ZY, Hu XJ (2008) Relationship between calcium decoding elements and plant abiotic-stress resistance. Int J Biol Sci 4(2):116–125. https://doi.org/10.7150/ijbs.4.116

Souza CR de, Morel JD, Santos AB M, da Silva WB, Maia VA, Coelho PA, Rezende VL, dos Santos RM (2019) Small-scale edaphic heterogeneity as a floristic–structural complexity driver in Seasonally Dry Tropical Forests tree communities. J For Res 31(6):2347–2357. https://doi.org/10.1007/s11676-019-01013-9

Sprent JI (2009) Legume Nodulation: A Global Perspective. John Wiley & Sons, Ltd. https://doi.org/10.1002/9781444316384

Terra M de C N S, Santos RM dos, Júnior JA do P, Mello JM de, Scolforo JR S, Fontes MA L, Schiavini I, Reis AA dos, Bueno IT, Magnago LF S, Steege H ter (2018) Water availability drives gradients of tree diversity, structure and functional traits in the Atlantic-Cerrado-Caatinga transition, Brazil. J Plant Ecol 11(6):803–814. https://doi.org/10.1093/jpe/rty017

Tilman D (1999) The ecological consequences of changes in biodiversity: A search for general principles. Ecology 80(5):1455–1474. https://doi.org/10.1890/0012-9658(1999)080[1455:tecoci]2.0.co;2

Tiessen H, Moir JO (1993) Total and organic carbon. In: Carter MR (ed) Soil sampling and methods of analysis. Lewis Publishers, Boca Raton, FL, pp 187–199.

Tong T, Li Q, Jiang W, Chen G, Xue D, Deng F, Zeng F, Chen Z H (2021) Molecular evolution of calcium signaling and transport in plant adaptation to abiotic stress. Int J Mol Sci 22(22):12308. https://doi.org/10.3390/ijms222212308

Vitousek PM (1982) Nutrient cycling and nutrient use efficiency. Am Nat 119:553–572. https://doi.org/10.1086/283931

Vitousek PM (1984) Litterfall, nutrient cycling, and nutrient limitation in tropical forests. Ecology 65:285–298. https://doi.org/10.2307/1939481

Walker, AP, Beckerman, AP, Gu, LH, Kattge, J, Cernusak, LA, Domingues, TF, Scales, JC, Wohlfahrt, G, Wullschläger, SD, Woodward, FL (2015). The relationship of leaf photosynthetic traits – V_{cmax} and J_{max} – to leaf nitrogen, leaf phosphorus, and specific leaf area: a meta-analysis and modeling study. Ecol Evol 4, 3218–3235. https://doi.org/10.1002/ece3.1173

Wang Q, Yang S, Wan S, Li X (2019) The significance of calcium in photosynthesis. Int J Mol Sci 20:1353. https://doi.org/10.3390/ijms20061353

Weil RR, Brady NC (2017) The nature and properties of soils. 15th Edition. Pearson, New York

Wickham H (2016) ggplot2: Elegant graphics for data analysis. Springer, New York, USA

Wilkins KA, Matthus E, Swarbreck SM, Davies JM (2016) Calcium-mediated abiotic stress signaling in roots. Front Plant Sci 7:1296. https://doi.org/10.3389/fpls.2016.01296

Wu S, Hu C, Tan Q, Li L, Shi K, Zheng Y, Sun X (2015) Drought stress tolerance mediated by zinc-induced antioxidative defense and osmotic adjustment in cotton (Gossypium hirsutum). Acta Physiol Plant 37:167. https://doi.org/10.1007/s11738-015-1919-3

Zanne AE et al. (2009) Towards a worldwide wood economics spectrum. Dryad Digital Repository. https://doi.org/10.5061/dryad.234

Zomer, RJ, Xu, J, Trabucco, A (2022) Version 3 of the global aridity index and potential evapotranspiration database. Sci. Data 9, 1–15. https://doi.org/10.1038/s41597-022-01493-1.

Statements and declarations

Funding

This research is part of the '*Nordeste Project: New Science for a Neglected Biome*', funded by the São Paulo Research Foundation (FAPESP, grant 2015/50488-5), and the Natural Environment Research Council (Newton Fund/NERC, grants NE/N012488/1, NE/N012550/1, NE/N012526/1). ATB was supported by a doctoral fellowship from the Coordination for the Improvement of Higher Education Personnel (CAPES, Finance Code 001), and is currently a postdoctoral fellow at the Brazilian National Council for Scientific and Technological Development (CNPq, process no. 153713/2024-0). MMES is supported by CNPq (grant 308623/2021-5) and the Minas Gerais Research Foundation (FAPEMIG, grant APQ-03020-22). DC is

supported by the CNPq (Research Productivity Fellowship, grant 314187/2021-9) and the Rio de Janeiro Research Foundation (FAPERJ, Programa Jovem Cientista do Nosso Estado – 2022, grant 200.153/2023). LPCM is supported by CNPq (Research Productivity Fellowship, grant 306563/2022-8) and FAPESP (grant 2021/10639-5). TFD is supported by CNPq (Research Productivity Fellowship, grant 312589/2022-0).

Competing Interests

The authors declare that they have no known competing financial interests or personal relationships that could have appeared to influence the work reported in this paper.

Author contributions

All authors contributed to the study writing, review and editing. Conceptualisation: A. T. B. and J. L.; Methodology: A. T. B., J. L., C. A. Q., O. L. P., P. W. M., and V. A. M.; Fieldwork: A. T. B., D. C., P. W. M., I. A. C. C., M. M. E. S., M. S. B. M., R. M. S., T. S., R. C. M., T. C. S. O., C. B., M. M., A. C. M. M. A., M. F. F., D. M. R., V. F. S., P. M. S. R., J. O. S., E. V., R. T. P., O. L. P., J. L., and T. F. D.; Formal analysis: A. T. B.; Writing – original draft: A. T. B; Visualisation: A. T. B., and D. C.; Supervision: J. L., and T. F. D.; Funding acquisition: J. L., and T. F. D.

Data availability

Original vegetation and soil data are integrated into the *ForestPlots Network* (www.ForestPlots.net). High-resolution images of the voucher specimens are also publicly accessible through the *speciesLink* network of biodiversity collections (http://www.splink.org.br/).